Special Review

Nan Zhang, Siyuan Wang and Catherine C.L. Wong*

Proteomics research of SARS-CoV-2 and COVID-19 disease

https://doi.org/10.1515/mr-2022-0016
Received June 5, 2022; accepted July 6, 2022;
published online September 14, 2022

Abstract: Currently, coronavirus disease 2019 (COVID-19) is still spreading in a global scale, exerting a massive health and socioeconomic crisis. Deep insights into the molecular functions of the viral proteins and the pathogenesis of this infectious disease are urgently needed. In this review, we comprehensively describe the proteome of severe acute respiratory syndrome coronavirus 2 (SARS-CoV-2) and summarize their protein interaction map with host cells. In the protein interaction network between the virus and the host, a total of 787 host prey proteins that appeared in at least two studies or were verified by co-immunoprecipitation experiments. Together with 29 viral proteins, a network of 1762 proximal interactions were observed. We also review the proteomics results of COVID-19 patients and proved that SARS-CoV-2 hijacked the host's translation system, post-translation modification system, and energy supply system via viral proteins, resulting in various immune disorders, multiple cardiomyopathies, and cholesterol metabolism diseases.

Keywords: COVID-19 disease; proteomics research; SARS-CoV-2 particles.

The proteome of SARS-CoV-2 and the role of the constituent proteins in self-replication

Severe acute respiratory syndrome coronavirus 2 (SARS-CoV-2), known as an enveloped β-coronavirus, is the causative agent of coronavirus disease 2019 (COVID-19). SARS-CoV-2 encodes 29 proteins, 16 non-structural proteins (NSP1-16) [1–3], four structural proteins (Spike [S], Envelope [E], Membrane [M], and Nucleocapsid [N]) [3], and nine putative accessory factors (open reading frame [ORF] 3a, 3b, 6, 7a, 7b, 8, 9b, 9c/14, and 10) [1, 2]. These proteins make up the proteome of SARS-CoV-2 (Figure 1A).

The replication transcriptase complex (RTC) is composed of the Neuroserpin (NSP) 3 viral papain-like protease, the NSP5 protease (3CLPro), the NSP7-NSP8 primase complex, the NSP12 primary RNA-dependent RNA polymerase (RdRp), the NSP13 helicase triphosphatase, the NSP14 exoribonuclease, the NSP15 endonuclease, and the NSP10/NSP16 N7- and 2′O-methyltransferase [1–4]. Among them, the NSP12 RdRp is the central enzyme within RTC. It helps to polymerize and complement full- and partial-length RNA templates (negative sense RNA) for the nascent strand synthesis of positive sense RNA genomes and subgenomic RNA species [4–6]. The NSP13 helicase displays dsDNA helicase activity, which untwists the SARS-CoV-2 dsRNA into two single sRNA, making it suitable for RNA replication [7, 8]. NSP15 trims ss/dsRNA, leading to production of 2′-3′ cyclic phosphodiester and 5′-hydroxyl termini [8, 9]. NSP14, bearing 3′ to 5′ exonuclease activity, is responsible for proofreading during RNA replication, thus enhancing genome replication ability [4, 8]. NSP16 is a s-adenosylmethionine-dependent (nucleoside-2′-O)-methyltransferase [8]. The NSP10

Nan Zhang and Siyuan Wang contributed equally to this work.

***Corresponding author: Catherine C.L. Wong**, Department of Medical Research Center, State Key Laboratory of Complex Severe and Rare Diseases, Peking Union Medical College Hospital (Dongdan Campus), Chinese Academy of Medical Sciences & Peking Union Medical College, No. 1 Shuaifuyuan Wangfujing, Dongcheng District, Beijing 100730, P. R. China; and Tsinghua University-Peking University Joint Center for Life Sciences, Tsinghua University, Beijing 100084, P. R. China, E-mail: catclw321@126.com. https://orcid.org/0000-0002-6855-2798
Nan Zhang, Department of Medical Research Center, State Key Laboratory of Complex Severe and Rare Diseases, Peking Union Medical College Hospital, Chinese Academy of Medical Sciences & Peking Union Medical College, Beijing, P. R. China; Department of Radiation Oncology, College of Medicine, The Ohio State University, Columbus, OH, USA; and Center for Cancer Metabolism, Comprehensive Cancer Center, The Ohio State University, Columbus, OH, USA, E-mail: nzhangwe@163.com
Siyuan Wang, Department of Medical Research Center, State Key Laboratory of Complex Severe and Rare Diseases, Peking Union Medical College Hospital, Chinese Academy of Medical Sciences & Peking Union Medical College, Beijing, P. R. China, E-mail: wsy1015@163.com

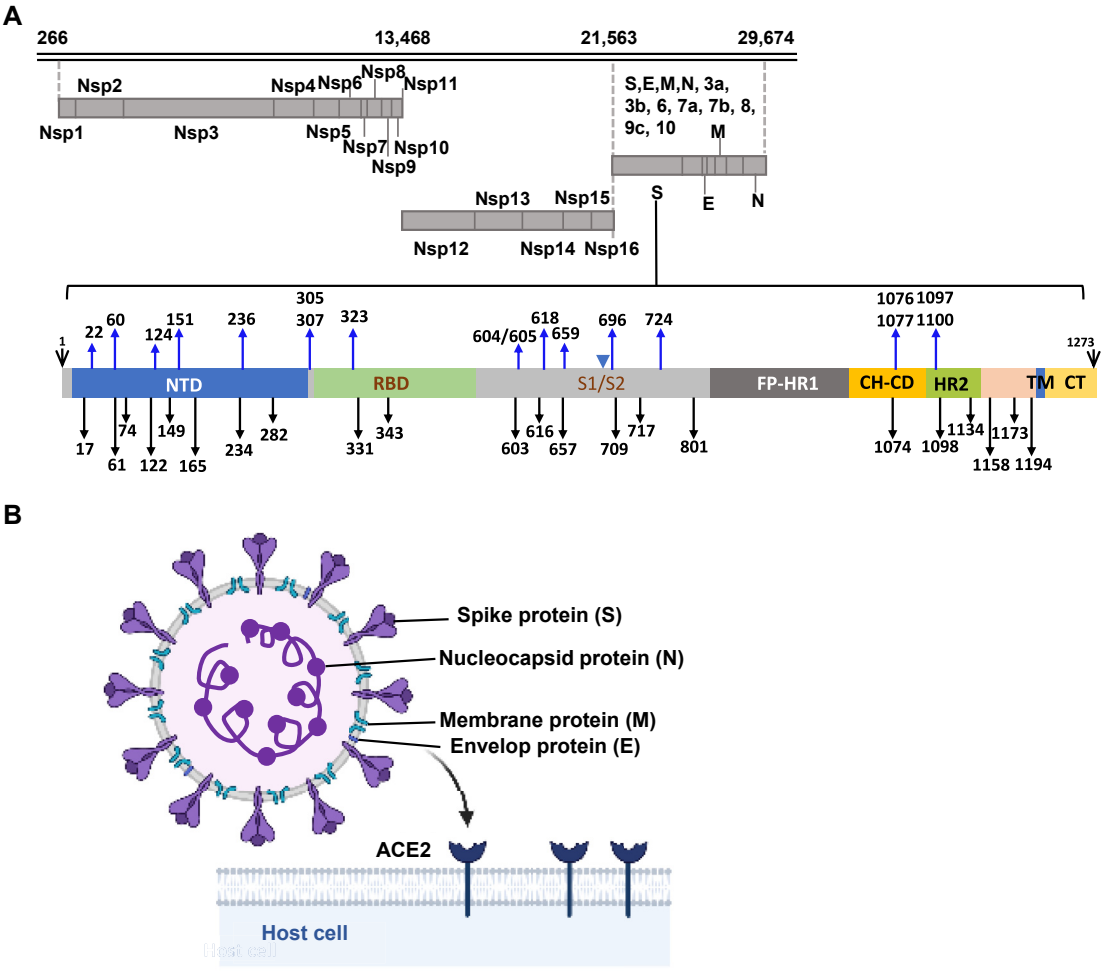

Figure 1: The severe acute respiratory syndrome coronavirus 2 (SARS-CoV-2) proteome.
(A) All proteins of SARS-CoV-2 and all glycosylation sites of the spike protein are shown. The black arrows indicate the N-glycosylation sites and the blue arrows show O-glycosylation sites. (B) Key features of SARS-CoV-2. ACE2, angiotensin-converting enzyme 2; CH, central helix: CD, connector domain: CT, cellular tail; E, Envelop protein; FP, fusion peptide; HR1, heptad repeat 1; HR2, heptad repeat 2; M, Membrane protein; N, Nucleocapsid protein; Nsp, nonstructural protein; NTD, N-terminal domain; RBD, receptor-binding domain; S, Spike protein; S1, spike protein subunit 1; S2, spike protein subunit 2; TM, transmembrane domain.

protein presents as the activating partner of both NSP14 and NSP16, aiding in the RNA replication process [8]. The complex of the SARS-CoV-2 NSP7–NSP8 hetero-tetramer primase plays a pivotal role in efficient NSP12 RNA-dependent RNA polymerase activity [8, 10]. NSP3 shares a cysteine protease, which functions in recognition and cleavage of the LXGG motif between NSP1 and NSP2, NSP2 and NSP3, and NSP3 and NSP4 [8]. It is noteworthy that the heterotypical interactions between NSP2 and NSP3 are indispensable in the induction process of the desired curvature in the endoplasmic reticulum (ER) membrane during the production of virulent spherical particles [11]. NSP5 is mainly responsible for processing the ORF1a/b-encoded polyproteins, acts as the key element in virus protein maturation [8, 12]. Other than these non-structural proteins, the RTC may also include host factors that work in coordination in the synthesis of viral RNA [5].

Like other coronaviruses, SARS-CoV-2 particles are composed of S, E, M, and N construct proteins (Figure 1B). S, E, and M proteins are embedded in the bilayer envelope on the virus' surface, while the N proteins bind the RNA genome in a spiral symmetric manner at the core of the virion, resembling beads on a string [4, 13–15]. These four structural proteins are essential in morphogenesis and assembly of SARS-CoV-2 [4]. The E protein is an intact membrane protein which mainly participates in the assembly, budding, envelope formation, and pathogenesis of the virus [11, 15]. The M protein is an N-linked glycosylated protein and presents in the highest amount out of all proteins in coronaviruses [16]. It

helps to bend the membrane to create a spherical structure encircling the ribonucleoprotein and serves as a scaffold for viral assembly [15]. Notably, the generation of infectious spherical particles is promoted by co-expression of the E and M proteins [11]. The N proteins predominantly participate in viral RNA synthesis and attach the viral genome to RTC, thus in charge of viral replication [10]. Protruding from the enveloping surface of the virus, the S proteins are essential for receptor recognition and cell entry mediation of the host [15]. The S proteins are homotrimeric class I transmembrane fusion proteins, with a molecular weight of about 600 kDa and composed of two functional subunits [17–19]. The S1 subunit consists of N-terminal domain, receptor binding domain (RBD), and a signal peptide, while the S2 subunit contains conserved fusion peptide, heptapeptide repeats 1 and 2, transmembrane domain, and cytoplasmic domain [13, 20] (Figure 1). SARS-CoV-2 utilizes cell surface receptor angiotensin-converting enzyme 2 (ACE2) as a prime receptor [14]. Firstly, RBD of S1 unit binds to cell surface receptor ACE2. Then furin protease-like protease cleaves the cleavage site between S1/S2 subunits, thus activating the conformational change of S protein to expose the S2 subunit. Next, the S2 subunit further induces virion fuse with the cell membrane and initiates virus entry [2, 3, 18–21].

The surface of the S proteins is highly glycosylated, composed of 22 N-linked glycans and 17 O-glycans (Figure 1A), making a big difference in inducing the host immune response [17, 19, 20, 22]. Among the 22 sites, eight sites are composed of a large number population of oligomannose-type glycans, while the other 14 sites are shaped by highly processed complex-type glycans [19, 20]. Of the 17 O-glycosylation sites identified with the S proteins extracted from the SARS-CoV-2 virions, 11 sites are located near glycosylated Asn. Mutations of N616 by site-directed mutagenesis on purified full-length wild-type S proteins completely abolished the O-glycosylation on T618. This suggests the possibility of an “O-Follow-N” rule, indicating the occurrence of O-glycosylation near the glycosylated Asn [19]. The glycosylated amino acid residue blocks the antibody recognition, thus enabling the virus to escape innate and adaptive immune responses [17, 22].

Location of SARS-CoV-2 proteins and their cellular interactions with the host proteome

Understanding the localization trace of viral proteins and virus-host protein interactions is very important for interpreting the behavior and pathogenesis of viruses in host cells at macro and molecular levels.

Confirmed subcellular localization of viral bait proteins

SARS-CoV-2 virus infects and enters cells to hijack the host cell mechanisms for self-replication. These viral proteins are located in diverse positions in the cell [14], and the distribution of these viral proteins at the subcellular level is related to their unique biological functions. Some studies have reported on the subcellular localization of different bait proteins in host cells. Although most localization information was found to be the same, there are some inconsistencies, possibly due to different methods and materials. Some localization results were only supported by one research study, and similar results have not been observed in other studies. As such, the localization results require further research and confirmation. Therefore, we summarized the results from six analyses of viral proteins [8, 14, 23–26] and the location results of virus baits were recognized by at least two researchers were analyzed (Figure 2). There were 10 baits (NSP4, NSP6, E, M, S, ORF6, ORF7a, ORF7b, ORF8, and ORF10) that showed an ER distribution, nine baits (NSP6, E, M, S, ORF3a, ORF3b, ORF6, ORF7a, and ORF8) that were associated with the Golgi apparatus, and one bait ORF3a that was associated with endosomes and lysosomes. Three baits (NSP6, NSP16, and ORF9b) were reported to be localized to the mitochondrion. Although coronavirus replication is most likely to occur in the cytoplasm of the host cells, 13 bait proteins (NSP1, NSP5, NSP6, NSP9, NSP10, NSP11, NSP13, NSP14, NSP15, NSP16, M, ORF7b, and ORF9c) were reported to have a nucleus-related location (Figure 2). Overall, the results provide a more comprehensive and accurate portrayal of the subcellular molecular context, which is essential for accurately understanding the activities of the viral proteins in the host cells.

A SARS-CoV-2 protein interaction map

Similar to how host proteins are constantly engaged in various life activities, the viral proteins that enter cells are also occupied with executing their duties instead of resting at only one position. There are stable, weak, and transient protein interactions between viral bait proteins and prey proteins in the host cells. Therefore, combining the affinity purification-mass spectrometry and proximity-based labeling biotin identification-mass spectrometry methods together can aid in comprehensively capturing virus–host interaction proteins. Moreover, it was inevitable that bait proteins captured some non-specific interaction proteins, which was a common flaw in the experiments.

Several studies [8, 14, 23, 27, 28] have focused on the virus–host interactions and identified thousands of prey proteins in the host cells. We summarized the interaction

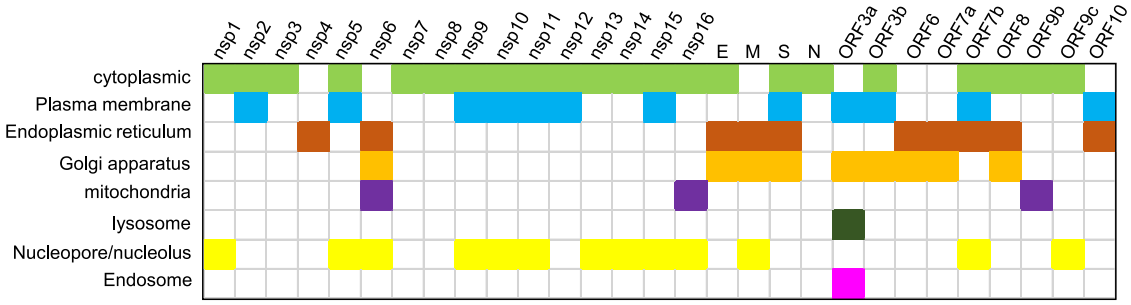

Figure 2: Confirmed subcellular localization of severe acute respiratory syndrome coronavirus 2 proteins in the host cell (same colors indicate exact locations). E, Envelop protein; M, Membrane protein; N, Nucleocapsid protein; Nsp, nonstructural protein; ORF, open reading frame; S, Spike protein.

results and found that 787 host prey proteins were identified in at least two studies or verified by co-immunoprecipitation experiments. These proteins interacted with 29 viral bait proteins and formed a network composed of 1,762 proximal interactions (Table 1). Two proteins, CD147 (BSG) [29] and transferrin receptor (TFRC) [30], are attractive as alternative receptors for SARS-CoV-2. We found that BSG interacts with viral protein M while TFRC interacts with nsp6, ORF3a, and ORF7. This indicates that SARS-CoV-2 may have other pathways of cell entry with the help of viral proteins M, nsp6, ORF3a, and ORF7. Furthermore, it is highly possible that virions can enter the cells by endocytosis with one or more of the three proteins nsp6, ORF3a, and ORF7 because TFRC mainly acts as an adaptor protein in the endocytosis biological pathway [31].

Hijacking of the ER system by SARS-CoV-2

Enrichment analysis of the Kyoto Encyclopaedia of Genes and Genomes (KEGG) pathway for all 787 proteins showed 45 prey proteins related to protein processing in the ER (Figure 3). Firstly, ribosomes are anchored on the ER by two ribosome anchor components, Oligosaccharyl transferase complex and Cytoskeleton-associated protein 4 (Climp63). Afterward, the newly synthesized peptides in the ribosomes are transported to the ER by Secretion (Sec) protein complex of Sec61-Sec62/63 acting as a translocon [32]. The newly synthesized peptides in the ER are N-glycosylated. These N-linked glycans increase the hydrophilicity of the modified proteins and are helpful for protein folding. After identification and folding with the help of lumenal chaperone proteins immunoglobulin heavy chain binding protein (Bip), Glucose-Regulated Protein (GRP) 94, Heat Shock Protein (HSP) 40, and a negative regulatory factor Hypoxia Up-Regulated Protein 1 (HYOU1), the outer two glycan molecules of the N-glycosylated peptides are hydrolyzed and cut off by glucosidases Neutral alpha-glucosidase AB (GANAB) and Glucosidase 2 subunit beta (PRKCSH) in the ER, indicating a folding process. Next, they mature with the help of dextran-dependent chaperone proteins Calnexin, Calreticulin, and Endoplasmic Reticulum Resident Protein 57 (ERp57) connected with monoglucosylated glycoproteins ER. The properly folded proteins are then packaged into

Table 1: Virus–host interaction proteins.

Bait	Prey-human
NSP1 (36)	NOP56, ARPC1B, RRP9, DKC1, AP2A1, ALDOA, KRT8, HNRNPC, RPSA, XRCC6, XRCC5, KRT10, FBL, ATP5F1D, KRT9, RPS19, LRPPRC, NOP2, RPS10, HNRNPM, ACTR3, RPS16, PRKDC, SRSF6, NOLC1, NUP93, COLGALT1, MYO18A, NUP205, ARPC1A, EIF3C, PKP2, PYM1, EFHD1, NAT10, NOP58
NSP2 (17)	SLC27A2, MT-CO2, COX7A2, POR, ATP5F1D, ACADVL, RAP1GDS1, ATP1B3, RAB10, NME3, NNT, RCN1, GIGYF2, VCPIP1, STOML2, DICER1, USP16, ACTN4
NSP3 (11)	MYO1C, HNRNPDL, MYO1B, MYO1D, ATP5F1D, FXR2, RHOA, RPL38, ACTC1, FMR1, ZER1
NSP4 (112)	NBAS, MYO1C, HGS, SLC27A2, SPTBN2, SEC16A, ARPC1B, TPD52L2, MYO1B, RRP9, WDR1, LRP6, FLOT1, TMCC1, ERLIN2, IPO7, AP2A1, LDHA, GLUD1, LMNA, ALDOA, OAT, GAPDH, TP53, RPN1, EIF2S1, KRT18, GPI, LDHB, P4HB, YES1, RPSA, DLD, CALM2, HSPA5, SLC25A6, PDIA4, HSP90B1, DSP, RCC1, LMNB1, MCM3, TARS1, CALR, MCM5, MYH10, LONP1, EIF4A3, RPS19, NAMPT, EMD, SERPINH1, LRBA, ARSL, NUP107, ARPC4, ACTB, ACTR3, SEC61A1, RPS16, H4C15, PPIA, RPL38, TMF1, PFKP, LMNB2, GOLGA3, ADAM9, DDX39B, DAG1, FLOT2, ITPR2, ITPR1, RAB35, SEC23A, INA, IMMT, GRIPAP1, PPP1R15B, CDC42BPA, NBEAL1, MON2, HOOK3, WDR75, PNPLA6, KCT2, USP32, TRPM4, PIGO, SCFD2, GBF1, MYO18A, ARPC1A, NEO1, USP7, GCC1, CLMN, VPS13A, PRR14, WDR11, ZDHHC5, NAT10, VPS33B, COG4, GPR108, CISD1, PI4KB, XPR1, SUCO, SLC25A10, SRP68, PIKFYVE, ARFGEF2
NSP5 (27)	MYO1C, SPTBN2, MYO1B, H2BC12, RPN1, TPM1, DLD, TOP1, SNRPB, RPL35A, MYL12A, SDHA, MCM4, MYH10, LRPPRC, EMD, HNRNPM, ACTR2, RPS16, RPL38, PRKDC, TFAM, SLC25A11, DDX39B, MYH14, GNB4, SUPT16H, HDAC2, TRMT1

Table 1: (continued)

Bait	Prey-human
NSP6 (181)	ATP5MG, ILVBL, GPR89A, PGRMC1, SLC33A1, NDUFA4, TP53I11, SCAMP3, XPO1, SPTBN2, SCAMP2, ARPC2, PGRMC2, SURF4, YKT6, GPAA1, HNRNPR, ADCY9, WDR1, SEC22B, TACC1, NUP155, ZMPSTE24, ATP5PD, ERLIN2, VAPB, GCNT3, SEC24B, ACSL3, TOMM40, CYB5A, CYB5R3, PNP, MT-ATP6, LMNA, TFRC, HMGCR, GAPDH, RPN1, RPN2, ATP1A1, EIF2S1, ATP5F1B, LDHB, SRPRA, PDHA1, DLD, UCHL1, CALM2, CD99, PRKCSH, PKM, SNRPB, UQCRB, POR, PTPN1, ARF4, RCC1, ATP2B1, RAB6A, LMNB1, ATP5PB, MCM3, ATP5F1A, MSN, RPL10, CANX, MARCKS, PRDX3, ATP5F1D, PPP2R1A, SDHA, MYH10, ETFB, EIF4A3, ARL1, EIF2S3, LRPPRC, VDAC2, ATP5PO, LMAN1, SERPINH1, RAB5C, SSR4, ALDH3A2, HSD17B4, ATP1B3, ATP5MF, TMEM33, ARPC4, RAB8A, RAB2A, RAB10, ACTR3, RHOA, RPS16, TRA2B, AP2B1, RPL38, TFAM, CLTC, SLC7A5, PFKP, SLC25A11, CKAP4, GOLGA3, CHAF1B, STIM1, DDX39B, FKBP8, GANAB, EMC2, RAB3GAP1, SLC39A14 (mitochondria), OXA1L, RAB35, ELAVL1, SLC1A5, ATP6AP1, IMMT, YIF1B, RABL3, DHRS7B, MRPL14, HACD2, COX15, KCTD9, ATG9A, KTN1, VKORC1L1, NUP93, GHDC, SLC35F6, EMC1, ATAD1, RETREG2, USP32, NUP35, TOR1AIP2, MOSPD2, NUP210, SYNE2, NCLN, CCDC47, SYAP1, LRRC59, AP2M1, CERS2, VMP1, CDK5RAP3, PIGS, CLCC1, TTC1, SIGMAR1, YIPF4, ALG1, PTDSS2, SGPP1, OSBPL8, SLIRP, LSG1, RAB1B, TMX1, ACBD3, PIGU, ATP13A3, GORASP2, POLR1B, TM9SF3, EMC7, SACM1L, MRPL16, TECR, EMC3, VAPA, DHCR7, SLC25A10, SEC63, WDR3, VDAC3, PTRH2, SRPRB, PFKP, DDOST
NSP7 (59)	POTEF, RABGAP1L, AGPS, MYO1C, PGRMC1, IPO5, XPO1, SPTBN2, ARPC1B, ARPC2, ARPC3, MYO1B, DPM1, H2BC12, MACROH2A1, ERLIN2, ACSL3, AP2A1, CYB5R3, RPN1, ATP1A1, SLC25A5, TPM3, LDHB, PDHA1, DLD, POTEJ, RALA, TOP2A, CKB, PDIA4, HSP90B1, UQCRB, ARF4, PDIA3, MCM4, LONP1, ETFB, MARCKSL1, FXR2, RAB5C, RAB7A, RAB8A, RAB2A, RAB10, ACTR2, RHOA, GNB1, TRA2B, RPL38, SLC7A5, PFKP, SRSF1, ILF2, CHAF1B, GANAB, KARS1, MRPL14, NCKAP5L, RAB18
NSP8 (20)	PGRMC1, IPO5, SEC22B, ATE1, LDHB, DLD, DLAT, MCM7, PHB, DLST, MARCKSL1, ATP5MF, RHOA, PPIA, TRA2B, PFKP, HERC1, MRPL14, YTHDF1, HECTD1
NSP9 (28)	IPO5, NDUFA10, PSAP, GNAI3, MTHFD1, GTF2F2, MCM7, CTNNA1, DDOST, FXR2, ATP1B3, CDC42, SEC61A1, SLC7A5, FMR1, PRPF4B, HSD17B12, NUP54, CAND1, CCAR1, NEK9, BBX, MAP7D2, SETD2, RAB1B, SFXN1, STOML2, VDAC3
NSP10 (20)	PGRMC1, IPO5, ARPC2, ARPC3, ERLIN2, AP2A2, LDHB, RPSA, DLD, TOP2A, UQCRB, RAB6A, MARCKSL1, FXR2, ATP5MF, RAB10, PFKP, AP2M1, NTPCR, GRPEL1
NSP11 (5)	PPIA, PGRMC1, ALB, KRT10, KRT2
NSP12 (13)	PDIA3, BAG2, PGRMC1, DNAJA2, PFDN1, SLC25A5, KRT18, CLTA, KRT10, KRT2, LONP1, STUB1, MYCBP2, PFKP, MYO1C, PGRMC, MYO1B
NSP13 (16)	ABLIM1, EIF2S1, KRT18, PCMT1, RRM2, STIP1, RDX, YAP1, TLE1, TLE3, GOLGA3, GOLGB1, GRIPAP1, PDE4DIP, ERC1, GCC2, NKB, DDX39B
NSP14 (13)	ALB, RPN1, EIF2S1, KRT18, KRT10, UBA1, STIP1, YAP1, CLTC, PEG10, CEP192, WDCP, SIRT5, MYO1C, MYO1B, GLO1, DDX39B
NSP15 (21)	MYO1C, CKB, MYO1D, RHOA, KARS1, RCN1, ALB, KRT8, TOP1, YWHAQ, CANX, MYH9, MYH10, KRT2, VDAC2, PRKDC, CLTC, GANAB, HAGH, DNAJA3, RBM14, MYO1B, APP, PDIA4
NSP16 (19)	DNAJA2, TTC4, BAG2, ALB, KRT10, PDIA4, PDIA3, STIP1, LRPPRC, DHPS, RPS16, RPL38, ELOB, GRIPAP1, WASHC2A, ERC1, PIBF1, YTHDF1, IBTK, PFKP, MYO1C, MYO1B
ORF3a (99)	PGRMC1, SCAMP3, HGS, ARPC1B, YKT6, ACTN4, SNX2, WDR1, SEC22B, ZMPSTE24, CPD, MYO1D, VAPB, SEC24B, TOMM40, CYB5A, CYB5R3, PNP (cytoplasm), TFRC, HLA-A, RPN1, ATP1A1, APP, EIF2S1, P4HB, YES1, GNAI3, CNP, U2AF1L5, CALM2, DLAT, CD99, PRKCSH, HSP90B1, ATP2A2, ARF4, CANX, NDUFS1, EPHA2, ATP5F1D, STIP1, MCM5, EIF2S3, RPS27, LRPPRC, VDAC2, MARCKSL1, SERPINH1, RAB5C, SSR4, VCP, TMEM33, EIF4A1, CDC42, RAB8A, SEC61A1, RPS16, RAB1A, DYNLL1, DYNLT1, BASP1, TFAM, CLTC, SLC7A5, PFKP, GOLGA3, DDX39B, DSG2, GANAB, PDIA6, MLF2, HSD17B12, NEDD1, HM13, CCDC47, SYAP1, DNAJA3, VPS39, TRAPPC9, H2AC1, MCCC1, CLCC1, TUBB6, LSG1, RAB1B, VPS16, VPS11, ACBD3, GOPC, SACM1L, TECR, VAPA, SLC25A10, SUN2, RAB21, MYO6, VDAC3, HYOU1, YTHDF2, SUPT16H, PFKP, PDIA4, CALR, DDOST, CKAP4
ORF3b (50)	MYO1C, SPTBN2, ARPC1B, ARPC2,STX7, BUB3, ZMPSTE24, STAM2, MYO1D, ERLIN2, NDUFA10, AP2A1, LMNA, TP53, RPN1, P4HB, TPM1, CALM2, PDIA4, ETFA, HSP90B1, SNRPB, UQCRB, NDUFV2, CANX, ATP5F1D, ATP5F1C, VDAC2, STT3A, MARCKSL1, RAB10, ACTR2, FAU, PPIA, TRA2B, PRKDC, CLTC, SPTBN1, SRSF1, GOLGA3, DDX39B, DSG2, GANAB, ARFGAP2, RBM14, EFHD1, YTHDF1, RAB1B, TECR, STOML2, VDAC3
ORF6 (39)	NUP98, MYO1C, YKT6, NUP155, MYO1D, SEC31A, VAPB, PCNT, RPN1, KRT10, ETFA, SNRPB, LMNB1, CANX, HNRNPH3, KRT2, EIF2S3, VDAC2, QARS1, LMAN1, EMD, H4C15, AP2B1, RAE1, PRKDC, SPTBN1, PFKP, PPP2R3A, GOLGA3, KARS1, RCN1, UBR4, GCC2, TFG, BORCS6, RBM14, TRIM56, GRPEL1, RAI14, LEMD3
ORF7a (123)	ILVBL, PGRMC1, SCAMP3, HGS, SLC27A2, SEC16A, YKT6, XPOT, RANBP6, FAM20B, WDR1, SEC22B (endoplasmic reticulum – Golgi), TACC1, NUP155, ZMPSTE24, STAM2, CPD, LTN1, ERLIN2, VAPB, SEC24B, ACSL3, CYB5A, LMNA, TFRC, ALDOA, OAT, RPN1, RPN2, ATP1A1, LDHB, P4HB, CALM2, PDIA4, POR, ATP2A2, PTPN1, ARF4, LMNB1, CAD, CALR, CANX, NDUFS1, ATP5F1D, MCM5, MDH2, VDAC2, STT3A, MARCKSL1, LMAN1, EMD, FXR2, RAB5C, RAB7A, RAB27A, SSR4, BCAP31, SEC24C, NAPA, ATP5ME, RAB8A, RAB2A, HSPE1, PPIA, TMF1, CLTC, PFKP, SLC25A11, LMNB2, CKAP4, GOLGA3, GOLGA2, NNT, DDX39B, DSG2, FKBP8, RAB35, ELAVL1, IMMT, PDS5A, RABL3, REEP3, MON2, MTDH, KTN1, NUP93, ARFGAP2, ATAD1, KCT2, NUP35, TOR1AIP2, HM13, NUP210, SCFD2, SCFD1, USP7, NCLN, CCDC47, SYAP1, LRRC59, DDRGK1, COG3, LSG1, TMX1, ACBD3, GORASP2, XPO5, PREB, ATP13A1, SACM1L, MDN1, FANCI, ATAD3A, ARL8B, TECR, VAPA, DHCR7, DNAJB11, SEC63, SRP68, NDUFA12, STUB1, VDAC3, PSAT1

Table 1: (continued)

Bait	Prey-human
ORF7b (149)	GPR89A, SLC33A1, STX16, TNFRSF10B, SCAMP3, SCAMP1, SCAMP2, TM9SF1, STX7, GPR39, CA12, ADCY9, PRAF2, SLC43A1, ZMPSTE24, MYO1D, CTDNEP1, LMNA, ALB, ALDOA, OAT, EIF2S1, TPM3, H2BC11, LDHB, ANXA2, YES1, MET, RPSA, HNRNPA1, MGST1, PCNA, EEF2, KRT10, CD99, PRKCSH, HSP90B1, SNRPB, GJA1, LMNB1, PCMT1, CFL1, MCM3, TARS1, CANX, EPHA2, PRDX3, HNRNPH3, KRT2, ACVR1B,EIF4A3, IL6ST, EIF2S3, VDAC2, RPS10, IQGAP1, STT3A, QARS1, LMAN1, SLC26A2, RAB5C, RAB7A, RAB13, VAMP7, ARFIP1, SEC61B, ACTB, DAD1, H4C15, RAB1A, RACK1, BASP1, EFNB1, CLTC, SPTBN1, NRG1, GOLGA3, STX4, PTPRJ, STX5, TCIRG1, SPTAN1, DDX39B, FKBP8, GANAB, MFSD10, KARS1, PDIA6, ATP6AP1, SGCB, CYP1B1, HAGH, IMMT, ALG11, ANO6, LPCAT4, STEAP3, RHBDD2, TMEM214, TMEM205, LCLAT1, LRIG3, SCARA5, ERMP1, LRP10, ADGRG6, TRIM59, SLC15A4, TMEM87A, RNF149, C5orf15, NETO2, DAGLB, GPRC5A, TRPM4, SCARB1, SLC35F5, AHCTF1, SYMPK, DDX17, NEO1, USP7, RFT1, TMEM159, TLCD1, RBM14, PHB2, PRXL2A, NDFIP1, TMEM70, STRA6, LGR4, TMX1, GORASP2, GRPEL1, VEZT, ITM2C, ABCB10, GINM1, ZDHHC18, TMOD3, GPRC5B, LRFN1, ADD3, SRP68, NOTCH3, MYO6, MYRF, ZDHHC9, PTRH2
ORF8 (137)	PGRMC1, PLOD2, NOP56, TOR1A, TOR1B, ARPC2, ARPC3, ACTN4, MYO1B, SYNCRIP, PLOD3, SEC22B, MYO1D, ERLIN2, VAPB, LDHA, C5, TGFB1, FGA, FGB, OAT, GAPDH, TP53, RPN1, RPN2, ITGB1, TPM3, H2BC11, P4HB, RPSA, HNRNPA1, U2AF1L5, CALM2, DLAT, TOP1, MTHFD1, PCNA, SLC25A6, ACTN1, PDIA4, PRKCSH, PKM, HSP90B1, SNRPB, UQCRB, POR, IGFBP3, LMNB1, VDAC1, GART, PPIB, CFL1, MCM3, CALR, CANX, ERP29, PRDX3, PDIA3, HNRNPH3, ETFB, EIF4A3, EIF2S3, VDAC2, RPS10, STT3A, LMAN1, TUFM, SERPINH1, SSR4, YARS1, CSE1L, TMEM33, ARPC4, ACTB, ACTR3, ACTR2, RHOA, TGFB2, RPS16, CNBP, TRA2B, RACK1, TPM4, SPTBN1, PFKP, PLOD1, CKAP4, SRSF1, MFGE8, TRAP1, NME3, SRSF6, OS9, ADAM9, SPTAN1, DDX39B, FKBP8, GANAB, LTBP1, PDIA6, PPA1, RCN1, NPTX1, SRSF7, DBN1, MAN2A1, HAGH, HSD17B12, ACTBL2, POGLUT2, YTHDF3, ERO1B, PLD3, EMC1, GGH, DDX17, RBM14, PHB2, AIF1L, EFHD1, RBM4, SRRT, EDEM3, TMX1, SMOC1, SFXN1, TMOD3, UGGT2, TECR, SAE1, DNAJB11, MRTO4, MYO6, VDAC3, CFL2, HYOU1, YTHDF2, FKBP7
ORF9b (54)	MYO1C, IPO5, SPTBN2, ARPC3, NDUFS2, NDUFS3, ATP5PD, TOMM70, AP2A2, NDUFA10, CYB5R3, OAT, EIF2S1, ATP5F1B, PDHA1, CALM2, DLAT, MTHFD1, ETFA, COX6B1, UQCRC2, ATP5F1A, MARK3, PRDX3, SDHA, MCM4, SHMT2, PHB, DLST, ETFB, MDH2, LRPPRC, ATP5MF, NDUFA6, ACTR3, TFAM, PFKP, OGDH, SSBP1, TRAP1, NME3, FKBP8, KARS1, OXA1L, NDUFA9, TIMM50, MARK2, DLG5, TBRG4, PHB2, HSD17B10, TOMM22, OCIAD1, MARK1, POLDIP2
ORF9c (23)	MYO1C, P4HB, PDIA4, ERLIN2, PDIA3, TPM3, RPSA, KRT10, HSP90B1, HNRNPL, PCMT1, ATP5F1D, PHB, MYH10, KRT2, HNRNPA3, PRKDC, SSBP1, PRDX4, HAGH, DDX17, HSD17B10, POLDIP2
ORF10 (72)	PGRMC1, SURF4, SMARCA5, MYO1D, ERLIN2, VAPB, AHSA1, LMNA, OAT, RPN1, P4HB, RPSA, CALM2, PCNA, PDIA4, ETFA, PRKCSH, VDAC1, TCEA1, PPIB, MCM3, CALR, CANX, PRDX3, HNRNPH3, LONP1, ETFB, EIF4A3, DDOST, VDAC2, ATRX, MARCKSL1, LMAN1, FXR2, HSD17B4, PGD, YARS1, CSE1L, RHOA, CNBP, TRA2B, NUCB2, CLTC, PFKP, YWHAH, CKAP4, GANAB, PDIA6, PPA1, SRSF7, BEND3, CTR9, YTHDF3, CAND1, TXNDC5, IPO4, SCFD1, BBX, DDX17, ZNF512B, IPO9, RBM14, PARK7, NAT10, TMOD3, UGGT1, USP36, SAE1, DNAJB11, RAB21, MYO6, CNPY2, YTHDF2
N (17)	ANKRD17, ALDOA, UBA1, NDUFS1, STIP1, SHMT2, G3BP1, TRIM25, RC3H1, YTHDF3, UPF1, TTC1, MOV10, IGF2BP1, G3BP2, TNRC6B, R3HDM2, PGRMC, TDRD3
E (69)	AP3B1, PGRMC2, YKT6, SNX2, DKC1, MYO1D, SEC31A, VAPB, LMNA, GAPDH, TP53, RPN1, TPM3, H2BC11, ANXA2, KRT19, GNAI3, RPSA, TPM1, DLD, DBT, SLC25A6, PDIA4, LMNB1, CANX, PRDX3, PDIA3, STIP1, MCM5, HSPA4, EIF2S3, LRPPRC, VDAC2, RPS10, ARCN1, EMD, ACTB, RPS16, RPL23, TPM4, CLTC, SPTBN1, PFKP, YWHAH, SSRP1, GANAB, KARS1, RAB11B, SRSF7, HAGH, NDUFA9, ZC3HAV1, YTHDF3, NUP93, NUP35, USP7, AP2M1, RBM14, PHB2, ESYT1, LSG1, ACBD3, GORASP2, GRPEL1, ATAD3A, MRPL16, SNX6, POLDIP2, YTHDF2, SUPT16H, PGRMC, MYO1B
S (56)	PGRMC1, CDIPT, YKT6, TRIM13, DNAJA2, MYO1D, ERLIN2, VAPB, CYB5R3, LMNA, GAPDH, TP53, RPN1, RPN2, TPM3, HNRNPA1, PDIA4, HSP90B1, PTPN1, ARF4, LMNB1, VDAC1, PCMT1, CANX, PDIA3, HNRNPH3, EIF2S3, VDAC2, RPS10, EMD, TMEM33, RAB10, RPS16, H4C15, PPIA, RACK1, PRKDC, SLC25A3, PFKP, CKAP4, PDIA6, SLC9A3R2, IMMT, SLC27A3, RPS27L, ZC3HAV1, GOLGA7, AP2M1, SDF2, CDCA3, ZDHHC5, LSG1, SDF2L1, TECR, HACD3, VAPA, HYOU1, MYO1C, MYO1B, HSPA5, DDX39B
M (226)	ILVBL, GPR89A, HAX1, PGRMC1, CDIPT, HGS, SLC27A2, PLXNB2, PGRMC2, SURF4, SLC16A4, YKT6, MYO1B, SLC37A4, ICMT, SNX2, DPM1, PRAF2, SEC22B, PMPCB, ERLIN1, NUP155, STAM2, CPD, SLC22A5, LTN1, MYO1D, ERLIN2, USP19, YIF1A, VAPB, SEC24B, ACSL3, BAG2, AIFM1, FADS2, LMNA, GAPDH, RPN1, RPN2, ATP1A1, ATP1B1, SLC25A5, PCCB, EIF2S1, ITGB1, EPHX1, LDHB, HNRNPC, SLC3A2, GNAI3, CALM2, SLC25A6, CKB, PDIA4, CD99, PKM, HSP90B1, SNRPB, ATP2A2, HSPA6, PFKL, PTPN1, RPL35A, ARF4, SLC9A1, ATP2B1, RAB6A, LMNB1, COMT, STOM, CANX, PPP2R1A, SLC7A1, SDHA, DNAJA1, STIP1, MCM5, BSG, GGCX, EIF4A3, RPS19, DDOST, ARL1, USP8, HADHA, EIF2S3, RPS27, VDAC2, RPS5, IQGAP1, LMAN1, EMD, SERPINH1, LRBA, SSR4, ALDH3A2, SLC25A1, AP2S1, ATP1B3, SLC12A2, HADHB, TMEM33, ARPC4, UBE2G2, CDC42, RAB10, ABCE1, RHOA, RPS16, RAB1A, PPIA, AP2B1, DYNLL1, RPL38, PRKDC, ATP2C1, CLTC, REEP5, SLC7A5, PFKP, SLC25A11, CAV1, TAP2, ARHGAP1, GOLGA3, NME3, STIM1, SPTAN1, DSG2, GANAB, SLC39A14, KARS1, RHEB, DHCR24, SEC23B, ELAVL1, SLC1A5, HAGH, IMMT, ANO6, HSD17B12, USP39, PYCR3, YIF1B, PITRM1, SLC27A3, ODR4, UBR4, CDKAL1, MICOS13, LMBRD2, TTC27, CNNM4, MTHFD1L, METTL7B, LRIG3, RPS27L, COX15, ZFYVE16, MON2, KTN1, VRK2, RHOT1, ST13P4, MACO1, RETREG2, CNNM3, SLC30A7, LPCAT1, TOR1AIP2, ATL2, CIP2A, SMAP2, FAR1, SYNE2, AHCTF1, GBF1, ABCC2, YIPF5, CCDC47, SYAP1, FERMT2, FAF2, COQ8B, DNAJA3, CYFIP2, INTS4, DDRGK1, CDK5RAP3, VPS13A, ERGIC2, CLCC1, OSBPL9, PHB2, SDF4, TUBGCP2, ESYT1, ALG1, OSBPL11, YTHDF1, OSBPL8, WDR11, DDX47, RAB1B, SPNS1, ACBD3, GRPEL1, VEZT, RTN4, FANCI, TMEM160, TECR, VAPA, DHCR7, DNAJB11, STOML2, AMFR, STUB1, SNX6, VDAC3, FNDC3A, LEMD3, ALG6, CEPT1, SLC4A7, SEC23IP, XPO1, IPO5

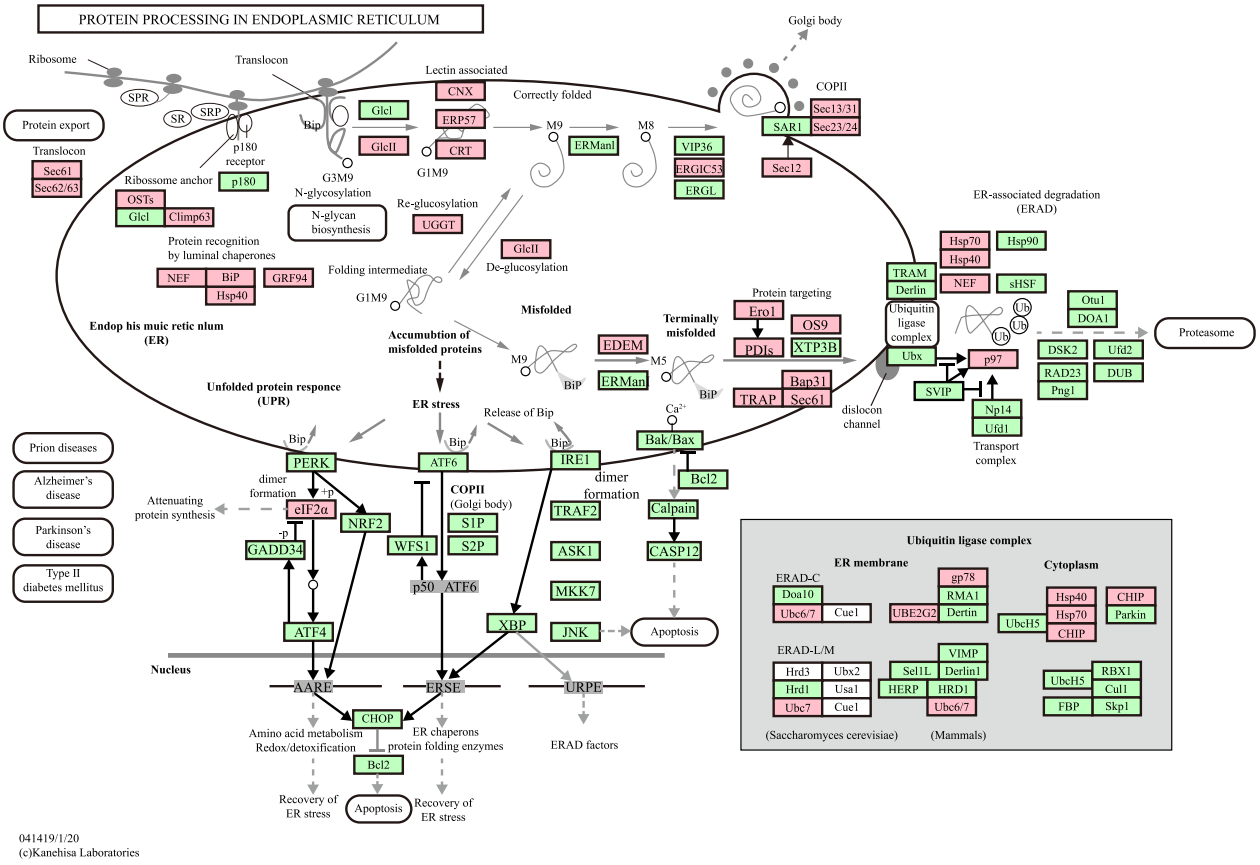

Figure 3: Kyoto Encylopaedia of Genes and Genomes pathway enrichment analysis of 787 prey proteins interacting with viral baits. The red color represents prey proteins involved in protein processing in the endoplasmic reticulum. The red color represents prey proteins involved in protein processing in the endoplasmic reticulum. AARE, Acylamino-acid-releasing enzyme; ATF4, activating transcription factor 4; ATF6, activating transcription factor 6; ASK1, Apoptosis signal-regulating kinase 1; Bap31, B-cell receptor-associated protein; Bak/Bax, Bax and Bak are members of the Bcl-2 family and core regulators of the intrinsic pathway of apoptosis; Bcl2, BCL2 Apoptosis Regulator; BiP, bingding protein, an ER-mediated chaperone; CASP12, caspase 12; CHIP, E3 ubiquitin ligase; CHOP, C/EBP-homologous protein; CNX, Calnexin; COPII, the Coat Protein Complex II; CRT, calreticulin; Cul1, Cullin 1; Cue1, coupling of ubiquitin conjugation to ER degradation protein 1; Climp63; Doa10, an ubiquitin ligase complex; DOA1, a Cdc48 cofactor Ufd3; DSK2, Ubiquitin domain-containing protein DSK2; DUB, deubiquitinating enzymes; eIF2α, eukaryotic Initiation Factor 2; EDEM, ER degradation-enhancing alpha-mannosidase-like protein 3; ER, endoplasmic reticulum; ERAD, ER-associated degradation; FBP, folate Binding protein; Glcl, glucosidase I; GlcII, glucosidase II; GRP94, heat shock protein 90 kDa; G1M9, Glc1Man9GlcNAc2 (G1M9); GADD34, Growth arrest and DNA damage-inducible protein 34; gp78, glycoprotein 78; G3M9, Glc3Man9GlcNAc2; Hsp, Heat shock 70-kDa protein; Hrd, HMG-CoA reductase degradation; HERP, homocysteine-induced endoplasmic reticulum protein; HRD1, an E3 Ubiquitin ligase involved in degradation of proteins; IRE1, the Inositol-requiring enzyme 1; JNK, c-Jun N-terminal kinase; NEF, nucleotide exchange factors; NRF2, the nuclear factor erythroid 2–related factor 2; Npl4, component of transport complex; OS9, osteosarcoma-9; Otu1, Ubiquitin thioesterase; OSTs, the oligosaccharyl transferases; PDIs, protein disulphide isomerases; p50-ATF6, transcriptionally active transcription factor 6; p97, the ATP-driven chaperone valosin-containing proteinvalosin-containing protein; p180, ribosome receptor; PERK, protein kinase R-like ER kinase; Png1, an N-glycanase; RBX1, E3 ubiquitin-protein ligase RBX1; RMA1, E3 Ubiquitin-protein ligase RNF5; RAD23, UV excision repair protein RAD23; SVIP, Small VCP/p97-interacting protein; Skp1, S-phase kinase associated protein 1; Sel1L, SEL1L Adaptor Subunit Of ERAD E3 Ubiquitin Ligase; Sec, Secretion; SAR1, an Arf family small GTPase; sHSF, heat shock protein; SPR, signal recognition protein; SR, serine/arginine-rich protein; TRAF2, TNF Receptor Associated Factor 2; TRAP, translocon-associated protein, a transport messenger on the endoplasmic reticulum membrane; TRAM, translocating chain-associated membrane protein; UbcH5, Human Ubiquitin-Conjugating Enzyme E2 D1; UBE2G2, Ubiquitin-conjugating enzyme E2 G2; Ub, ubiquitin; Ubc, ubiquitin C; Ufd, ubiquitin fusion degradation protein; Ubx, Ubiquitin-associated domain-containing ubiquitin regulatory X; UGGT, UDP-glucose glycoprotein glucosyltransferase; Usa1, a scaffold of the HRD-ubiquitin ligase; URPE, unfolded response pathway element; UPR, Unfolded protein responce; VIP36, Vesicular integral-membrane protein VIP36; VIMP, VCP-interacting Membrane Protein; WFS1, Wolfram syndrome 1 protein; XTP3B, endoplasmic reticulum lectin 1; XBP, X-box-binding protein.

transport vesicles and shuttled to the Golgi complex with the help of the ER-Golgi intermediate compartment (ERGIC) marker ERGIC53, Sec12, Sec13/31, Sec23/24, which are also required for the formation of the Coat Protein complex II transport vesicles from the ER. Some misfolded N-glycosylated proteins can be glycosylated by UDP-glucose glycoprotein glucosyltransferase UGGT (UGGT1, UGGT2). Thus they can be connected with Calnexin and Calreticulin to be refolded a second time. The other misfolded proteins are cut off with a mannose residue by ER degradation-enhancing alpha-mannosidase-like protein 3 (EDEM3), preventing them from obtaining the correct confirmation and resulting in terminally misfolded proteins, which bind to the ER chaperone BiP and are directly degraded by the proteasome in ER-associated degradation. Finally, they are transferred to ubiquitin ligase complex in ER with the help of ERO1-like protein, protein disulfide isomerases, The protein "amplified in osteosarcoma-9" (OS-9), B-cell receptor-associated protein 31 (Bap31), HSP75, and Sec61.

In the interaction network, we found six compounds of ubiquitin ligase complex –Ubiquitin-conjugating enzyme E2 G2 (UBE2G2), E3 ubiquitin–protein ligase (AMFR), DnaJ homolog subfamily A member 2 (DnaJA2), DnaJ homolog subfamily A member 1 (DnaJA1), Heat shock 70-kDa protein 6 (HSPA6), E3 ubiquitin-protein ligase CHIP (STUB1). Transitional ER ATPase and two accessory proteins binding ubiquitinated proteins were essential for the export of misfolded proteins from the ER to the cytoplasm, and BAG family molecular chaperone regulator 2 (BAG2) acted as a nucleotide exchange factor, which facilitates the release of adenosine diphosphate from HSP70 and Heat Shock Cognate protein 70 (HSC70) proteins, resulting in triggering of client/substrate protein release.

Ten viral proteins (ORF8, M, ORF7a, ORF10, NSP6, ORF7b, S, NSP4, E, and ORF6) interacted with the 45 prey proteins located in ER according to Nathe above conclusion. According to one study, another two viral proteins, ORF9c and ORF3a, interacted with the above host proteins based on observations in ER by confocal microscopy [14, 24]. The consistency between the microscopy results and interaction studies provides further evidence that SARS-CoV-2 hijacked the host ER system, possibly through the 12 viral proteins interacting with the 45 host proteins.

We also found that there were other viral bait proteins (ORF3b, NSP7, NSP12, NSP16, NSP15, NSP9, NSP14, NSP5) that interacted with the 45 host proteins, and ER locations have not been reported for these proteins. For protein processing in the ER, fewer interaction proteins have these viral protein pathways; NSP5 and NSP14 have only one, NSP9 and NSP15 have only two interacting proteins. We speculate that there may only be transient interactions between these proteins, which makes it difficult to observe their existence under a microscope. The lower number of interacting proteins may lead to a greater probability of false positives.

Hijacking of phagocytosis by SARS-CoV-2

Phagocytosis, one of the first processes that responds to infection, is a primary mechanism of the innate immune defense. Human angiotensin-converting enzyme 2 (hACE2) is a known receptor for SARS-CoV-2 in the process of cell entry through endocytosis [33, 34]. Fifteen prey proteins from the interaction network are involved in the Phagocytosis pathway (Figure 4). Five of those proteins, ras-related protein Rab-7a (RAB7A), Transferrin receptor protein 1 (TFRC), HLA class I histocompatibility antigen, An alpha chain (HLA-A), Scavenger receptor class B member 1 (SCARB1), and 1-phosphatidylinositol 3-phosphate 5-kinase (PIKFYVE), are involved with identification and entry of SARS-CoV-2. ACE2 is essential in the early stages of viral entry. Previous research studies have shown that loss of RAB7A may sequester the ACE2 receptor inside the cells, leading to reduced viral entry [35]. TFRC is an alternative receptor for SARS-CoV-2 entry [30]. HLA-A is an antigen-presenting primary histocompatibility complex class I (MHCI) molecule with immunodominant epitope originated from SARS-CoV-2 [36]. Hence, it is not difficult to speculate that HLA-A is a key element in SARS-CoV-2 recognition through the phagocytosis pathway. SCARB1 facilitates the entry of SARS-CoV-2 by acting as an entry co-factor through high-density lipoprotein (HDL) binding [37]. PIKFYVE is necessary for cell entry of SARS-CoV-2 by endocytosis and potentially a universal drug target for viruses entering cells via endocytosis [34]. PIKFYVE is also essential for maturing early endosomes into late endosomes, phagosomes, and lysosomes in the phagocytosis pathway [38]. Integrin beta-1 (ITGB1) is another phagocytosis-promoting receptor.

There are another 11 proteins that play roles in the phagocytosis pathway and participate in phagosome formation, phagolysosome formation, and cross-presentation. Hepatocyte growth factor-regulated tyrosine kinase substrate (HGS) is reported to be engaged in intracellular signal transduction. Ras-related protein Rab-5C (RAB5C), SEC22B-Vesicle-trafficking protein (SEC22B), Syntaxin-7 (STX7), protein transport protein Sec61 subunit alpha isoform 1 (SEC61A), and protein transport protein Sec61 subunit beta (SEC61B) mediates the endocytic trafficking or protein transport [38–43]. Calnexin (CANX)/Calreticulin (CALR) is a calcium-binding chaperone abundant within ER. CALR mainly performs functions in protein assembly, promotion

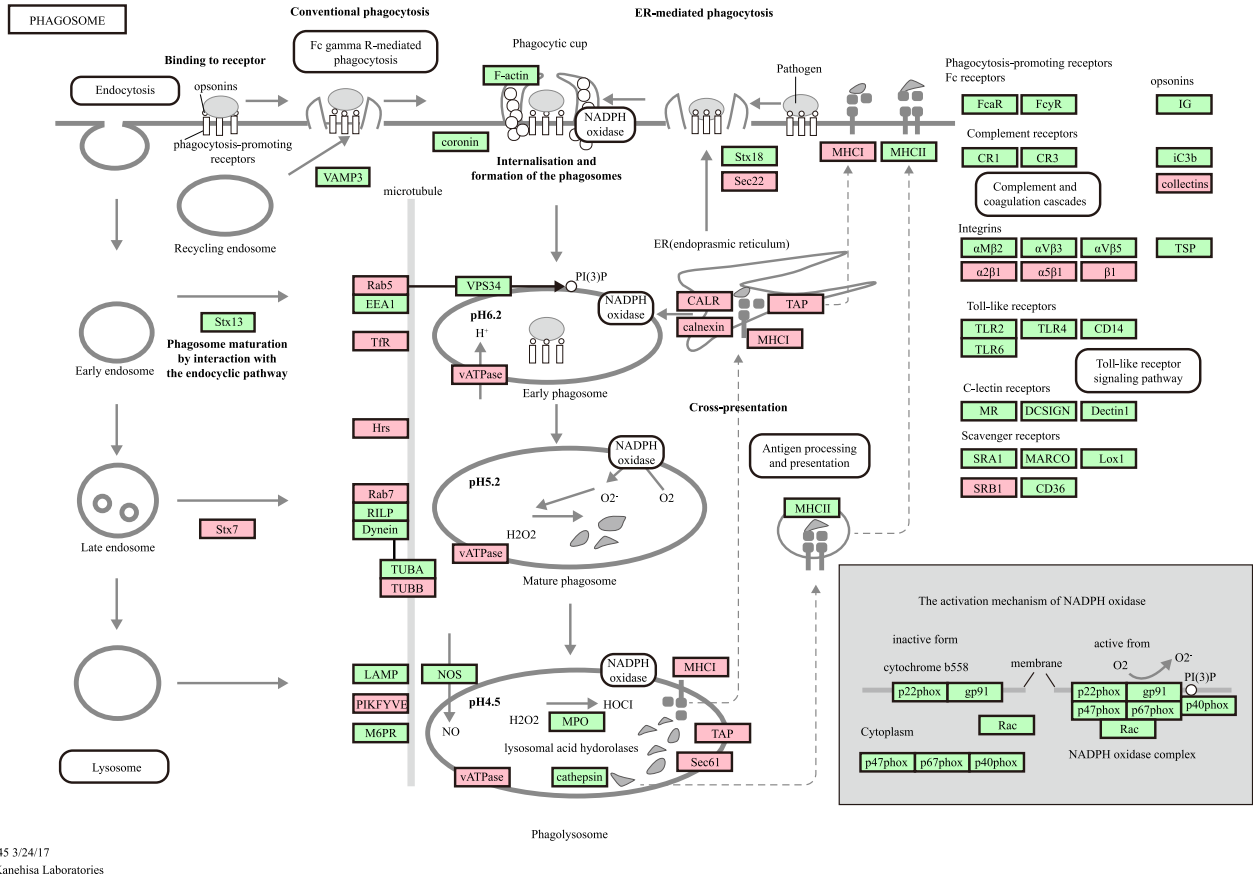

Figure 4: Kyoto Encylopaedia of Genes and Genomes pathway enrichment analysis of 787 prey proteins interacting with viral baits. The red color represents prey proteins involved in phagocytosis. The red color represents prey proteins involved in phagocytosis. CALR, Calreticulin; DCSIGN, a C-type lectin receptor; EEA1, early endosome antigen 1; ER, endoprasmic reticulum; FcaR, Fc alpha receptor; FcyR, Fc receptors for IgG; gp91, a NADPH oxidase subunit; Hrs, the ESCRT-0 subunit HRS; iC3b, a protein fragment that is part of the complement system, a component of the vertebrate immune system; IG, immunoglobulin; LAMP, the lysosomal membrane proteins; Lox1, Lectin-like oxidized low-density lipoprotein (LDL) receptor-1; M6PR, mannose-6-Phosphate Receptor; MPO, human Myeloperoxidase; MHCI, primary histocompatibility complex class I; MHCII, the major histocompatibility complex class II; MR, C-type lectin receptors; MARCO, mreceptor with collagenous structure; NADPH, reduced nicotinamide adenine dinucleotide phosphate; NOS, nitric oxide synthase; NO, Nitric oxide; PIKFYVE, 1-phosphatidylinositol 3-phosphate 5-kinase; PI(3)P, Phosphatidylinositol 3-phosphate; Rab5, Ras-related protein 5; Rab7, Ras-related protein Rab-7; Rac, ras-related C3 botulinum toxin substrate; RILP, Rab-interacting lysosomal protein; Sec22, Secretion 22; SRA1, steroid Receptor RNA Activator 1; SRB1, the Scavenger Receptor Class B type 1; TAP, Antigen peptide transporter 2; TfR, transferrin receptor; TLR, Toll-like receptors; TSP, thrombospondin, an integrin-associated protein; TUBA, tubulin alpha chain; TUBB, Tubulin beta; VAMP3, vesicle associated membrane protein 3; vATPase, v-type ATPase; VPS34, class III phosphoinositide 3-kinase.

of unassembled protein subunits retention within the ER, or viral protein processing. Antigen peptide transporter 2 (TAP2) is associated with antigen processing. TAP2 is indispensable in both of peptide-MHCI assembly and antigen presentation [44–47]. An adequate supply of peptide antigens binding with MHCI molecules requires the presence of TAP1 and TAP2 [44, 45]. Tubulin beta-6 chain (TUBB6), V-type proton ATPase 116 kDa subunit a 3 (TCIRG1), and V-type proton ATPase subunit S1 (ATP6AP) are three other proteins that assist in phagocytosis.

Proteins interacted with viral bait proteins (ORF3a, ORF7b, ORF7a, NSP6, M, NSP4, ORF8) and most of the proteins involved in phagocytosis, indicating that SARS-CoV-2 hijacked phagocytosis through these bait proteins after entering host cells, thereby achieving the purpose of avoiding the innate immune response. Other viral proteins, NSP7, ORF3DEPB, ORF10, ORF6, E, S, NSP8, NSP9, and NSP15, have less than two interacting proteins in this pathway and need further research to address the high probability of false positives.

Hijacking of the oxidative phosphorylation pathway of host cell by SARS-CoV-2

Components of the oxidative phosphorylation system are located on the mitochondria' inner membrane. The system is composed of five complexes: Nicotinamide adenine dinucleotide (NADH) dehydrogenase complex (Complex I), Succinate dehydrogenase complex (Complex II), Cytochrome *bc*1 complex (Complex III), Cytochrome *c* oxidase complex (Complex IV), and the ATP synthase (Complex V). In the protein interaction network of the host cell with SARS-CoV-2, there are 22 participants distributed in all the complexes of the oxidative phosphorylation pathway (Figure 5). NADH-ubiquinone oxidoreductase 75 kDa subunit (NDUFS1), NADH dehydrogenase [ubiquinone] iron-sulfur protein 2 (NDUFS2), NADH dehydrogenase [ubiquinone] iron-sulfur protein 3 (NDUFS3), NADH dehydrogenase [ubiquinone] flavoprotein 2 (NDUFV2), NADH dehydrogenase [ubiquinone] 1 alpha subcomplex subunit (NDUFA)10, NDUFA12, NDUFA4, NDUFA6, NDUFA9 are nine subunits of Complex I. Cytochrome *c* oxidase assembly protein COX15 homolog (Cox15), Cytochrome *c* oxidase subunit 6B1 (COX6B1), Cytochrome *c* oxidase subunit 7A2 (COX7A2), and Cytochrome *c* oxidase subunit 2 (MT-CO2) are four subunits of Complex IV. ATP synthase subunit alpha (ATP5F1A), ATP synthase subunit beta (ATP5F1B), ATP synthase subunit gamma (ATP5F1C), ATP synthase subunit delta (ATP5F1D), ATP synthase subunit e (ATP5ME), ATP synthase subunit a (MT-ATP6), V-type proton ATPase 116 kDa subunit a 3 (TCIRG1), and V-type proton ATPase subunit S1 (ATP6AP1)

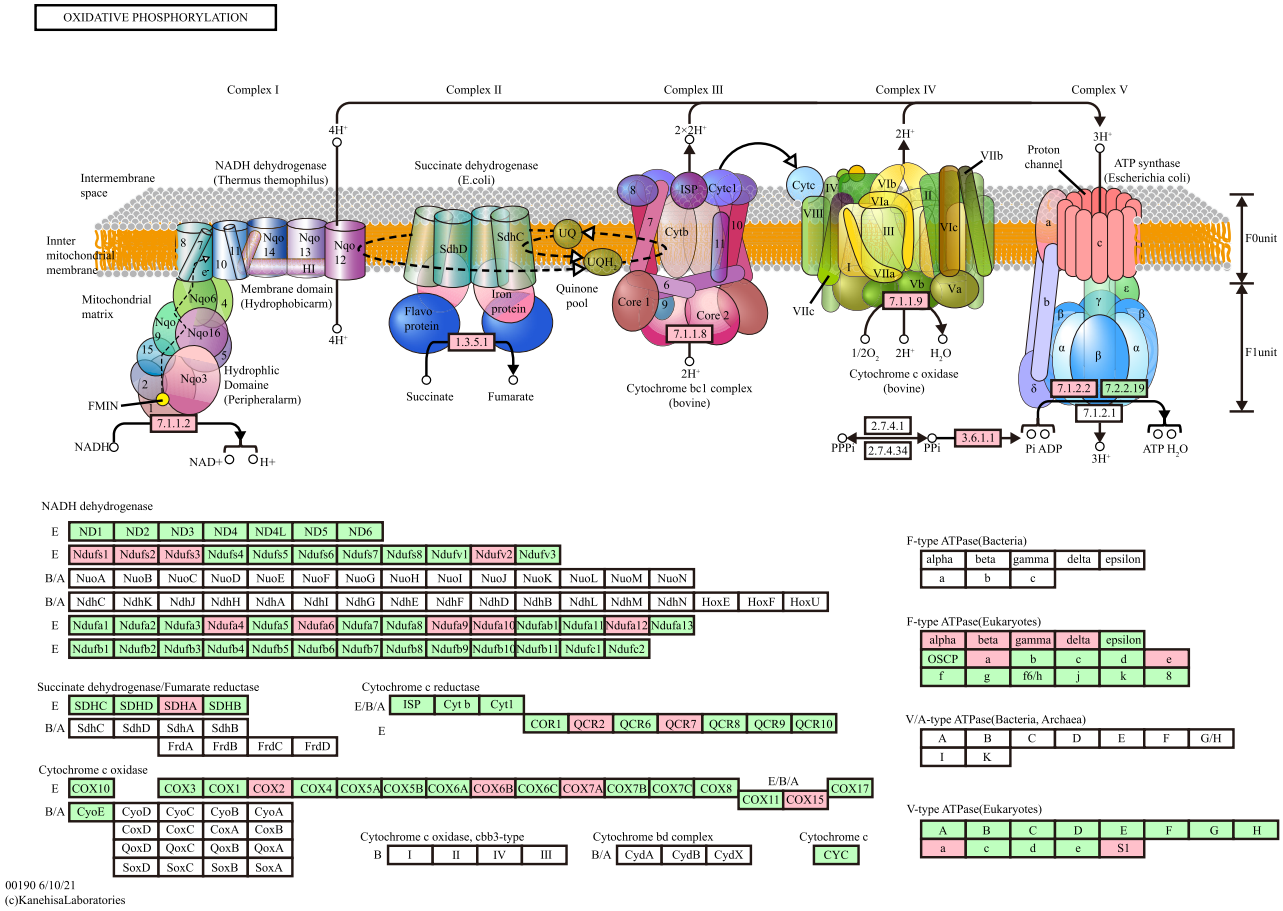

Figure 5: Kyoto Encylopaedia of Genes and Genomes pathway enrichment analysis of 787 prey proteins interacting with viral baits. The red color represents prey proteins involved in protein processing in oxidative phosphorylation. The red color represents prey proteins involved in protein processing in oxidative phosphorylation. ATP, adenosine triphosphate; COR1, cytochrome-c reductase subunit COR1; COX, cytochrome c oxidase; CYC, Cytochrome c; Cyd, cytochrome bd-type quinol oxidase subunits; FMN, flavin mononucleotide; FrdA, a flavoprotein, part of an enzyme complex; FrdB, an iron-sulfur protein, part of an enzyme complex; Hox, hox hydrogenase; ISP, iron sulfur protein; NADH, Nicotinamide adenine dinucleotide; OSCP, oligomycin sensitivity-conferring protein; PPi, diphosphate; PPPi, tributylphosphoric acid; Pi, inorganic Phosphate; ADP, adenosine diphosphate; QCR, cytochrome c reductase; Qox, quinol oxidases; Sox, sulphur oxides protein; UQ, ubiquinone.

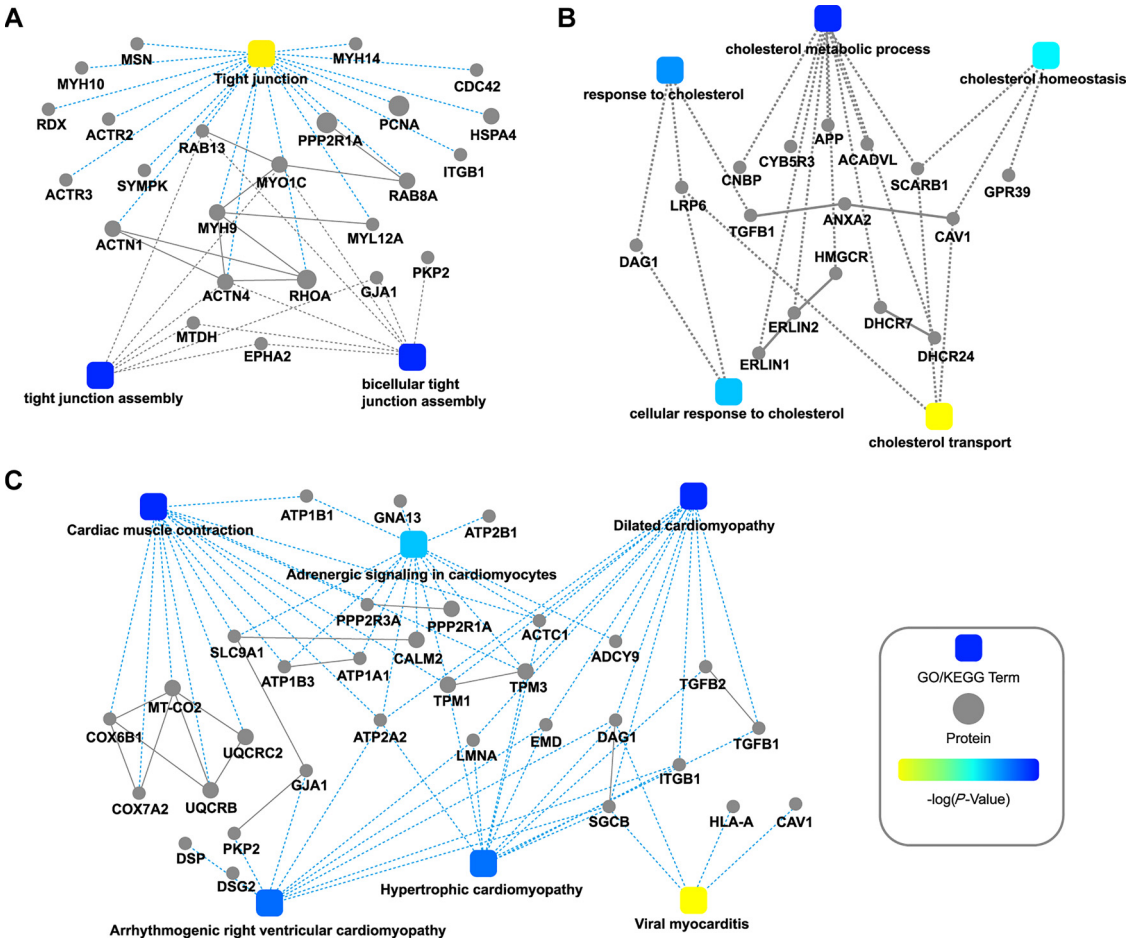

Figure 6: Functional analysis of host proteins interacting with the severe acute respiratory syndrome coronavirus 2 proteome.
(A) Interaction diagram for proteins involved in tight junctions (TJs) and TJs assembly-related pathways. Viral protein interactions are displayed in the top of the figure. (B) Interaction diagram for proteins involved in cholesterol-related pathways. (C) Interaction diagram for proteins involved in the pathways of cardiac muscle-related diseases. The gray dotted lines represent gene ontology (GO) pathways; blue dotted lines represent Kyoto Encylopaedia of Genes and Genomes pathways. The significance of the pathways is represented by –log(*P*-value) (Fisher's exact test) and is shown by color scales with dark blue indicating the highest level of significance. ACADVL, very long-chain specific acyl-CoA dehydrogenase; ACTC1, actin-alpha cardiac muscle 1; ACTR, antibody-coupled T cell receptor; ACTN, alpha-actinin; ADCY9, adenylate cyclase type 9; ANXA2, Annexin A2; APP, amyloid-beta precursor protein; ATP1A1, ATPase subunit alpha-1; ATP2A2, ATPase 2; ATP1B1, ATPase subunit beta-1; ATP1B3, sodium/potassium-transporting ATPase subunit beta-3; ATP2B1, plasma membrane calcium-transporting ATPase 1; CALM2, calmodulin-2; CAV1, Caveolin-1; CDC42, cell division control protein 42 homolog; CNBP, CCHC-type zinc finger nucleic acid binding protein; COX6B1, Cytochrome c oxidase subunit 6B1; COX7A2, Cytochrome c oxidase subunit 7A2; CYB5R3, NADH-cytochrome b5 reductase 3; DAG1, dystroglycan 1; DHCR, dehydrocholesterol reductase; DSP, 22-Desmoplakin; DSG2, desmoglein-2; EMD, Emerin; ERLIN1, Erlin-1; ERLIN2, Erlin-2; EPHA2, Ephrin type-A receptor 2; GJA1, gap junction alpha-1 protein; GNA13, guanine nucleotide-binding protein subunit alpha-13; GO, gene ontology; GPR39, G-protein coupled receptor 39; HLA-A, HLA class I histocompatibility antigen, An alpha chain; HMGCR, 3-Hydroxy-3-methylglutaryl-coenzyme A reductase; HSPA4, Heat shock 70-kDa protein 4; ITGB1, Integrin beta-1; KEGG, the Kyoto Encyclopaedia of Genes and Genomes; LRP6, Low-density lipoprotein receptor-related protein 6; LMNA, Prelamin-A/C; MSN, Moesin, membrane-organizing extension spike protein; MYH, myosin; MYO1C, unconventional myosin-Ic; MYH9, myosin-9; YL12A, transposon Ty1-LR2 Gag polyprotein; MTDH, NADP-dependent mannitol dehydrogenase; MT-CO2, cytochrome c oxidase subunit 2; PPP2R1A, serine/threonine-protein phosphatase 2A 65 kDa regulatory subunit A alpha isoform; PPP2R3A, serine/threonine-protein phosphatase 2A regulatory subunit B'' subunit alpha; PKP2, plakophilin-2; PCNA, proliferating cell nuclear antigen; RDX, radixin; RAB, ras-related protein Rab-7a; RHOA, transforming protein RhoA; RAB8A, ras-related protein Rab-8A; SCARB1, Scavenger receptor class B member 1; SGCB, beta-sarcoglycan; SLC9A1, sodium/hydrogen exchanger 1; SYMPK, Symplekin; TGFB1, transforming growth factor beta-1 proprotein; TGFB2, transforming growth factor beta-2 proprotein; TPM1, tropomyosin alpha-1 chain; TPM3; UQCRB, Cytochrome b-c1 complex subunit 7; UQCRC2, Cytochrome b-c1 complex subunit 2, mitochondrial.

are subunits of ATP synthase. Inorganic pyrophosphatase (PPA1) is the key enzyme that catalyzes the production of inorganic phosphates, and it is a synthetic substrate of ATP.

As mentioned above, the SARS-CoV-2 proteins NSP6, NSP16, and ORF9b are partly located in the mitochondrion of the host cell. Oxidative phosphorylation, a primary process occurring in the mitochondria, covers ORF9b and NSP6, which interacts with 10 and nine host cell proteins. This indicates that the two viral proteins, NSP6 and ORF9b, participate in hijacking the host cell's oxidative phosphorylation energy pathway. ORF7a, ORF3a, M, NSP7, and ORF9c have been reported to appear in mitochondria in only one research study each. We found that these proteins also appeared in the interaction network of the oxidative phosphorylation complex, which provided further evidence that they might be located in mitochondria. In the pathway, there were two or fewer proteins that interacted with the other bait proteins of SARS-CoV-2, ORF7b, ORF8, NSP1, NSP3, NSP5, NSP9, NSP10, ORF10, E, and N. There were five proteins that interacted with ORF3b, suggesting that ORF3b is located or partly located in the mitochondrion.

We can conclude that multiple viral proteins, especially NSP6 and ORF9b, hijacked the oxidative phosphorylation energy system of the host cell and likely led to dysregulation of mitochondrial functions [28]. Mitochondrial dysfunction is related to a variety of diseases, such as Parkinson's [48], Huntington's [49, 50], and Alzheimer's disease [48]. This may partly explain why patients infected with SARS-CoV-2 have neurological symptoms.

SARS-CoV-2 disturbed tight junction, cholesterol metabolic process, and cardiac muscle contraction process

In the protein interaction network of SARS-CoV-2 and the host cell, the host proteins participated in biological pathways related to tight junction (TJ), cholesterol, and cardiac disease are highly abundant (Figure 6A–C).

TJs contribute to establishing the epidermal permeability barrier by controlling the paracellular transport between neighboring cells. The destruction of TJs may pose a serious threat to health during virus infection [51]. The breakdown of the selective permeable barrier is reported to be closely associated with the hypoxemia in Acute Respiratory Distress Syndrome [52], representing one of the major risk factors affecting the case-fatality rate in COVID-19 patients [53, 54]. TJs have been reported to exist between epithelial cells in the lungs, intestines, kidney, and brain [55, 56]. Many of the host proteins in the interaction network are reported to be essential to TJs-related biological pathways. The Ras-related protein (RAB13) which regulates TJs assembly and activity, is conducive to establishing the Sertoli cell barrier [57–59] and may be related to cysts dispersed in cells lacking TJs [60]. Symplekin (SYMPK) is a specific component of the TJs plaque [61, 62]. Ephrin type-A receptor 2 (EPHA2) is associated with the positive regulation of bicellular TJ assembly [63] and Plakophilin-2 (PKP2) plays a role in junctional plaques [64]. There are at least three proteins interacting with the viral proteins ORF8 (7), NSP6 (6), ORF7b (5), M (4), NSP5 (4), ORF3a (4), NSP7 (3), and NSP15 (3) in TJs-related pathways according to the interaction network, as shown in Table 1.

Representing an essential component for mammalian cell functions and integrity, Cholesterol serves as a precursor of steroid hormones, bile acids, and vitamin D. The abnormal metabolism of cholesterol increases the risk for various endocrine disorders and cardiovascular diseases. Many host proteins that interact with the viral bait serve important biological functions in cholesterol-related processes. 3-Hydroxy-3-methylglutaryl-coenzyme A reductase (HMGCR), well-known as the main target of statins [65, 66], coordinates critical events in cellular cholesterol homeostasis [67–69]. Scavenger receptor class B member 1 (SCARB1) is the receptor for HDL. SCARB1 regulates selective uptake of HDL-associated cholesteryl ester and also facilitates the efflux of unesterified cholesterol [70]. Caveolin-1 (CAV1), Annexin A2 (ANXA2), and Low-density lipoprotein receptor-related protein 6 (LRP6) are involved with cholesterol transport [71–73]. Delta (24)-sterol reductase (DHCR24) and 7-dehydrocholesterol reductase (DHCR7) have important functions during the cholesterol biosynthesis process [74–79]. Erlin-1 (ERLIN1), Erlin-2 (ERLIN2), and CCHC-type zinc finger nucleic acid binding protein (CNBP) are involved in the regulation of cellular cholesterol homeostasis [80, 81]. More than three host proteins interacted with the viral proteins M, NSP6, NSP4, and ORF8, which may indicate that they play key roles in cholesterol related processes.

We also found that many of the prey proteins that interacted with SARS-CoV-2 are related to the physiology of cardiac muscles and the cardiac conduction system. Caveolin-1 (CAV1), plakophilin-2 (PKP2), calmodulin-2 (CALM2), tropomyosin alpha-1 chain (TPM1), and sodium/potassium-transporting ATPase subunit alpha-1 (ATP1A1) have been reported to be involved in cardiac muscle contraction [82–86]. Emerin (EMD), gap junction alpha-1 protein (GJA1), desmoglein-2 (DSG2) 22-Desmoplakin (DSP), and Sodium/potassium-transporting ATPase

subunit beta-1 (ATP1B1) are essential to cardiac conduction [87–92].

Prelamin-A/C (LMNA), transforming growth factor beta proprotein TGFB1 and TGFB2 relate to cardiac homeostasis, cardiac muscle cell differentiation and proliferation, respectively [87, 93–98]. The dysfunction of cytochrome *c* oxidase subunit 2 (MT-CO2), actin-alpha cardiac muscle 1 (ACTC1), sarcoplasmic/ER calcium ATPase 2 (ATP2A2), and sodium/hydrogen exchanger 1 (SLC9A1) would result in cardiomyopathy. The host prey proteins that are involved in the pathways of diseases related to the cardiac muscle also interacted with a series of viral proteins (at least three proximal interactions), such as M, NSP6, ORF3a, ORF7a, ORF8, nsp4, ORF3b, ORF7b, E, S, NSP2, NSP7, and ORF9b.

Previous research has shown that a number of proteins involved in TJ, cholesterol metabolic processes, and cardiac muscle contractions are disturbed after being infected with SARS-CoV-2 [99–101]. The fact that the host proteins interacted with the SARS-CoV-2 proteome through biological pathways further proves that the COVID-19 disease has disturbed the biological processes and provides an explanation for how this process occurred in cells.

Hijacking of the host cell translation process by SARS-CoV-2

By analyzing the interaction network, we found that SARS-CoV-2 interfered with the host cell's ribosome biogenesis process (XRCC5, XRCC6, PRKDC, NOP58, FBL, DKC1, and NAT10), nucleocytoplasmic transport (NUP205, NUP93, PYM1), and the formation of translation initiation complex (eIF3A) through nsp1 protein.

DNA-dependent protein kinase (DNA-PK) and nucleolar small ribosome particle core protein are related to ribosome biogenesis. DNA-PK include KU heterodimers (XRCC5, XRCC6) and a catalytic subunit DNA-PKcs (PRKDC). DNA-PK, which exists in the nucleolus in an rRNA-dependent manner, is purified together with small subunit processing bodies. The binding of KU to the end of the DNA strand may recruit and activate DNA-PKcs. KU drives the assembly of DNA-PKCs on U3 small nucleolar RNA, which is necessary for the processing of 18S rRNA.

Consist of Ku70 (XRCC5) and Ku80 (XRCC6), the Ku heterodimer may bind to DNA double-strand break ends, which is necessary for the non-homologous end joining of DNA repair pathway [102]. Fibrillarin (FBL), nucleolar protein (NOP58), and dyskerin (DKC1) are three core proteins that make up nucleolar ribosome particles. Small nucleolar (snoRNA) are located in the nucleolus, which guides the processing and modification of ribosomal RNA (rRNA) precursors and plays an important role in ribosome biogenesis. Studies have shown that the majority of snoRNP early stage processing and assembly occur in the nuclear plasma, which is transported to the nucleolus after assembly. RNA cytidine important transferase (nat10) is essential for the process of rRNA modification. The unique interaction of NSP1 with eIF3C (a component of the eIF3 translation initiation complex) causes translation inhibition via bridging mRNA to the small ribosomal subunit. Other studies demonstrated that NSP1 K164A and H165A mutations might block its interactions with eIF3 and small ribosomal subunits [23]. Four ribosomal proteins (RPS16, RPSA, RPS19, RPS10) were also found in these proteins, which further proved that NSP1 might interfere with the biogenesis or translation process of ribosomes. These processes occurred in the nucleus and cytoplasm, along with the microscopic localization of NSP1, further confirmed the authenticity of NSP1 virus protein functions in host cells.

Host response for COVID-19 infection

The wide clinical spectrum of COVID-19 disease ranges from asymptomatic to mildly symptomatic forms to severe clinical syndromes [103, 104]. In the most cases, patients will display an immune response without obvious symptoms within the first week of infection [105]. In COVID-19 and convalescent patients, the amount of down-regulated proteins was significantly more than that of up-regulated proteins, which led to a significant decrease in the number of identified proteins [99–101]. Contrary to the patients infected with SARS-CoV-2, there was a significant increase in the number of identified proteins in asymptomatic carriers, as compared to healthy controls [99, 101]. These proteins are involved in many aspects of the host response, which is helpful for deepening our understanding of the molecular mechanisms revealing COVID-19 infection.

Immune response

Increasing evidence illustrate that the progression of COVID-19 disease is highly associated with the host's immune response [106–109]. Considering the results from our research and other peer-reviewed publications, the immune response pattern of COVID-19 patients can be concluded as a multi-stage process: activation in the asymptomatic period, suppression in the mild/moderate period, abnormally activation in the severe period and prolonged suppression at convalescent period [99, 100].

We found that Dishevelled, EGL-10 and pleckstrin (DEP) along with a large number of proteins mainly involved in the innate immune response were highly enriched in asymptomatic carriers. Similarly, immune responses mediated by leukocyte and neutrophil were up-regulated. And cytokine production was also found to be increased [99]. On the contrary, the levels up-regulated proteins in the urine samples of asymptomatic carriers were mostly reduced in mild/moderate and severe patients. It was identified that proteins related to these functions switched from increase to decrease, indicating that the immune response changed from activation in asymptomatic infections to inhibition in symptomatic COVID-19 patients [99]. Some of the proteins were associated with neutrophil mediated phagocytosis, such as calpain (CAPN1), which is involved in neutrophil plasma membrane expansion in conjunction with cell spreading and phagocytosis [110–113]. Phagocytosis is one of the main mechanisms of the innate immune defense and it is one of the first processes that responds to infection. It has been reported that SARS-CoV-2 infections changed cell phagocytosis and neutrophilia in COVID-19 patients [114]. Peripheral neutrophil-to-lymphocyte ratio was also characterized to be increased in severe COVID-19 patients [115], suggesting that neutrophil degranulation may play a key role in modulating the landscape of immune changes after SARS-CoV-2 infection [116]. As a cytosolic protein involved in many biological processes, N-Myc downstream regulated gene 1 (NDRG1) mainly affected the differentiation process of macrophages [117]. The secretion of Macrophage migration inhibitory factor (MIF) in response to viral infections may trigger the production of inflammatory cytokines from T cells and macro-phages, eventually resulting in significant elevation in inflammatory response (also known as “cytokine storm”) [99, 100, 118]. Phagocytosis, mediated by neutrophils and macrophages, played a vital role during the whole COVID-19 disease development process, and it may be the SARS-CoV-2-specific risk factor determining the inflection point from asymptomatic to symptomatic [99].

Cholesterol metabolism

Cholesterol metabolism has been characterized to be directly involved in COVID-19 pathogenesis [99, 101, 119]. Previous studies suggest that HDL possess a protective action on the endothelial layer in COVID-19 patients [119]. Apolipoprotein A-I (ApoA1), known as an important member in HDL family, plays a crucial role for reverse cholesterol transport [99]. A number of studies have shown that ApoA1 is down-regulated throughout the disease cycle of COVID-19 [99–101]. The functional disorder of HDL serum may be indicative of the abnormalities in cholesterol reverse transport during SARS-CoV-2 infection.

Cardiac complications

Long-term myocardial disturbance is another feature of COVID-19. Myocarditis is a major cardiac complication found in COVID-19 BBA patients [106, 107, 120]. The rise of troponin I in the cardiac signaling correlates with a poor clinical outcome [99, 105]. The decrease of junction plakoglobin (JUP) in the serum of COVID-19 patients was found to be related to arrhythmic right ventricular cardiomyopathy (ARVC) [99]. Vascular function and coagulation pathways are also affected in the mild/moderate and severe COVID-19 stages [99]. The dysfunction is usually more serious in severe patients than in moderate patients, and this effect is extended until 6–12 months after recovery. The level of creatine kinase Myoglobin (MB) was reported to be significantly increased during convalescence, as compared with healthy controls. Arrhythmogenic right ventricular cardiomyopathy caused by the cascade reaction of complement and coagulation was also observed during convalescence [99, 101]. However, this phenomenon does not exist in asymptomatic infections, indicating little effect on the cardiovascular function or coagulation pathway [99].

Tight junction

With the exception of FZD5, the level of many proteins increased in the TJs assembly in asymptomatic carriers, but remarkably decreased in symptomatic COVID-19 patients [99, 100]. This indicates that TJs are partially activated in asymptomatic infections, while destructed during disease progression. The distinction in TJs variation at protein levels between the different infection periods indicated the occurrence of a defense process at the very early phase of infection [99].

Mitochondrion stress

Peroxiredoxin-3 (PRDX3) and carbamoyl phosphate synthase (CPS1) are two proteins which were found to be significantly elevated in the serum of COVID-19 patients. PRDX3, derived from mitochondria, is a known antioxidant. CPS1 is the main mitochondrial urea cycle enzyme in hepatocytes [121]. The proteins that were still affected 40–

60 days after virus infection were related with mitochondrial stress. This may indicate that mitochondrial stress reaction persists during SARS-CoV-2 infection.

Damage to other organs

There is compelling evidence that the infection of SARS-CoV-2 may result in multiple organ dysfunctions, covering the central nervous system, heart, gastrointestinal tract, kidney, liver, and muscle [82, 101, 105, 122–125].

The level of Cystatin C and progranulin was remarkably elevated in COVID-19 patients' serum. Notably, Cystatin C has been identified as an extracellular level biomarker for tumor, cardiovascular disease, and inflammatory lung disorders [126]. Progranulin appears to have a pro-inflammatory role in adipocytes in diabetes [127]. These results were shown with real-time architecture for autopsy samples collected from different organs of COVID-19 patients. It turned out that SARS-CoV-2 infection caused the dysregulation of more than 45% of total identified proteins in at least one organ/time point, indicating the devastating effect of the SARS-CoV-2 infection [128]. What is more striking is that the incidence of multiple organ dysfunction has actually increased among COVID-19 patients in the recovery stage [99].

Acknowledgments: We're grateful to Foreseen Biotech Ltd for their assistance in data analysis.
Research funding: This work is supported by Clinical Research Operating Fund of Central High level hospitals, Training Program of the Big Science Strategy Plan 2020YFE0202200, National Natural Science Foundation of China Grants 32150005, and Research Funds from Health@InnoHK Program launched by Innovation Technology Commission of the Hong Kong Special Administrative Region.
Author contributions: All authors have accepted responsibility for the entire content of this manuscript and approved its submission.
Competing interests: Authors state no conflict of interest.
Informed consent: Not applicable.
Ethical approval: Not applicable.

References

1. Wu F, Zhao S, Yu B, Chen YM, Wang W, Song ZG, et al. A new coronavirus associated with human respiratory disease in China. Nature 2020;579:265–9.
2. Chan JF-W, Kok K-H, Zhu Z, Chu H, To KK-W, Yuan S, et al. Genomic characterization of the 2019 novel human-pathogenic coronavirus isolated from a patient with atypical pneumonia after visiting Wuhan. Emerg Microb Infect 2020;9:221–36.
3. Fehr AR, Perlman S. Coronaviruses: an overview of their replication and pathogenesis. Methods Mol Biol 2015;1282: 1–23.
4. Feng W, Newbigging AM, Le C, Pang B, Peng H, Cao Y, et al. Molecular diagnosis of COVID-19: challenges and research needs. Anal Chem 2020;92:10196–209.
5. van Hemert MJ, van den Worm SH, Knoops K, Mommaas AM, Gorbalenya AE, Snijder EJ. SARS-coronavirus replication/ transcription complexes are membrane-protected and need a host factor for activity in vitro. PLoS Pathog 2008;4:e1000054.
6. Peng Q, Peng R, Yuan B, Zhao J, Wang M, Wang X, et al. Structural and biochemical characterization of the nsp12-nsp7-nsp8 core polymerase complex from SARS-CoV-2. Cell Rep 2020;31: 107774.
7. Jang KJ, Jeong S, Kang DY, Sp N, Yang YM, Kim DE. A high ATP concentration enhances the cooperative translocation of the SARS coronavirus helicase nsP13 in the unwinding of duplex RNA. Sci Rep 2020;10:4481.
8. Laurent EM, Sofianatos Y, Komarova A, Gimeno JP, Coyaud E. Global BioID-based SARS-CoV-2 proteins proximal interactome unveils novel ties between viral polypeptides and host factors involved in multiple COVID19-associated mechanisms. New York: Cold Spring Harbor Laboratory; 2020.
9. Yuen CK, Lam JY, Wong WM, Mak LF, Wang X, Chu H, et al. SARS-CoV-2 nsp13, nsp14, nsp15 and orf6 function as potent interferon antagonists. Emerg Microb Infect 2020;9:1418–28.
10. Zhai Y, Sun F, Li X, Pang H, Xu X, Bartlam M, et al. Insights into SARS-CoV transcription and replication from the structure of the nsp7-nsp8 hexadecamer. Nat Struct Mol Biol 2005;12:980–6.
11. Schoeman D, Fielding BC. Coronavirus envelope protein: current knowledge. Virol J 2019;16:69.
12. Macchiagodena M, Pagliai M, Procacci P. Identification of potential binders of the main protease 3CL(pro) of the COVID-19 via structure-based ligand design and molecular modeling. Chem Phys Lett 2020;750:137489.
13. Yao H, Song Y, Chen Y, Wu N, Xu J, Sun C, et al. Molecular architecture of the SARS-CoV-2 virus. Cell 2020;183:730–8.e13.
14. Liu X, Huuskonen S, Laitinen T, Redchuk T, Bogacheva M, Salokas K, et al. SARS-CoV-2-host proteome interactions for antiviral drug discovery. Mol Syst Biol 2021;17:e10396.
15. Satarker S, Nampoothiri M. Structural proteins in severe acute respiratory syndrome coronavirus-2. Arch Med Res 2020;51:482–91.
16. EA JA, Jones IM. Membrane binding proteins of coronaviruses. Future Virol 2019;14:275–86.
17. Bagdonaite I, Thompson AJ, Wang X, Søgaard M, Fougeroux C, Frank M, et al. Site-specific O-glycosylation analysis of SARS-CoV-2 spike protein produced in insect and human cells. Viruses 2021;13:551.
18. Walls AC, Park YJ, Tortorici MA, Wall A, McGuire AT, Veesler D. Structure, function, and antigenicity of the SARS-CoV-2 spike glycoprotein. Cell 2020;181:281–92.e6.
19. Tian W, Li D, Zhang N, Bai G, Yuan K, Xiao H, et al. O-glycosylation pattern of the SARS-CoV-2 spike protein reveals an "O-Follow-N" rule. Cell Res 2021;31:1123–5.
20. Watanabe Y, Allen JD, Wrapp D, McLellan JS, Crispin M. Site-specific glycan analysis of the SARS-CoV-2 spike. Science 2020; 369:330–3.

21. Sanda M, Morrison L, Goldman R. N- and O-glycosylation of the SARS-CoV-2 spike protein. Anal Chem 2021;93:2003–9.
22. Shajahan A, Supekar NT, Gleinich AS, Azadi P. Deducing the N- and O-glycosylation profile of the spike protein of novel coronavirus SARS-CoV-2. Glycobiology 2020;30:981–8.
23. Samavarchi-Tehrani P, Abdouni H, Knight J, Astori A, Gingras AC. A SARS-CoV-2 – host proximity interactome. New York: Cold Spring Harbor Laboratory; 2020.
24. Lee JG, Huang W, Lee H, van de Leemput J, Kane MA, Han Z. Characterization of SARS-CoV-2 proteins reveals Orf6 pathogenicity, subcellular localization, host interactions and attenuation by Selinexor. Cell Biosci 2021;11:58.
25. Zhang J, Cruz-Cosme R, Zhuang MW, Liu D, Liu Y, Teng S, et al. A systemic and molecular study of subcellular localization of SARS-CoV-2 proteins. Signal Transduct Target Ther 2020;5:269.
26. Gordon DE, Hiatt J, Bouhaddou M, Rezelj VV, Ulferts S, Braberg H, et al. Comparative host-coronavirus protein interaction networks reveal pan-viral disease mechanisms. Science 2020;370:eabe9403.
27. Gordon DE, Jang GM, Bouhaddou M, Xu J, Obernier K, White KM, et al. A SARS-CoV-2 protein interaction map reveals targets for drug repurposing. Nature 2020;583:459–68.
28. Stukalov A, Girault V, Grass V, Bergant V, Pichlmair A. Multi-level proteomics reveals host-perturbation strategies of SARS-CoV-2 and SARS-CoV. New York: Cold Spring Harbor Laboratory; 2020.
29. Wang K, Chen W, Zhang Z, Deng Y, Lian JQ, Du P, et al. CD147-spike protein is a novel route for SARS-CoV-2 infection to host cells. Signal Transduct Target Ther 2020;5:283.
30. Lai R, Tang X, Yang M, Duan Z, Peng X. Transferrin receptor is another receptor for SARS-CoV-2 entry. New York: Cold Spring Harbor Laboratory; 2020.
31. Bayati A, Kumar R, Francis V, McPherson PS. SARS-CoV-2 infects cells after viral entry via clathrin-mediated endocytosis. J Biol Chem 2021;296:100306.
32. Meyer HA, Grau H, Kraft R, Kostka S, Prehn S, Kalies KU, et al. Mammalian Sec61 is associated with Sec62 and Sec63. J Biol Chem 2000;275:14550–7.
33. Gheblawi M, Wang K, Viveiros A, Nguyen Q, Oudit GY. Angiotensin converting enzyme 2: SARS-CoV-2 receptor and regulator of the renin-angiotensin system. Circ Res 2020;126: 1456–74.
34. Ou X, Liu Y, Lei X, Li P, Mi D, Ren L, et al. Characterization of spike glycoprotein of SARS-CoV-2 on virus entry and its immune cross-reactivity with SARS-CoV. Nat Commun 2020;11:1620.
35. Daniloski Z, Jordan TX, Wessels HH, Hoagland DA, Kasela S, Legut M, et al. Identification of required host factors for SARS-CoV-2 infection in human cells. Cell 2021;184:92–105.e16.
36. Peng Y, Mentzer AJ, Liu G, Yao X, Yin Z, Dong D, et al. Broad and strong memory CD4(+) and CD8(+) T cells induced by SARS-CoV-2 in UK convalescent individuals following COVID-19. Nat Immunol 2020;21:1336–45.
37. Wei C, Wan L, Yan Q, Wang X, Zhang J, Yang X, et al. HDL-scavenger receptor B type 1 facilitates SARS-CoV-2 entry. Nat Metab 2020;2:1391–400.
38. Baranov MV, Bianchi F, Schirmacher A, van Aart MAC, Maassen S, Muntjewerff EM, et al. The phosphoinositide kinase PIKfyve promotes Cathepsin-S-mediated major histocompatibility complex class II antigen presentation. iScience 2019;11:160–77.
39. Meacock SL, Lecomte FJ, Crawshaw SG, High S. Different transmembrane domains associate with distinct endoplasmic reticulum components during membrane integration of a polytopic protein. Mol Biol Cell 2002;13:4114–29.
40. Lang S, Benedix J, Fedeles SV, Schorr S, Schirra C, Schäuble N, et al. Different effects of Sec61α, Sec62 and Sec63 depletion on transport of polypeptides into the endoplasmic reticulum of mammalian cells. J Cell Sci 2012;125:1958–69.
41. Haßdenteufel S, Johnson N, Paton AW, Paton JC, High S, Zimmermann R. Chaperone-mediated Sec61 channel gating during ER import of small precursor proteins overcomes Sec61 inhibitor-reinforced energy barrier. Cell Rep 2018;23:1373–86.
42. Chitwood PJ, Hegde RS. An intramembrane chaperone complex facilitates membrane protein biogenesis. Nature 2020;584: 630–4.
43. Schubert D, Klein MC, Hassdenteufel S, Caballero-Oteyza A, Yang L, Proietti M, et al. Plasma cell deficiency in human subjects with heterozygous mutations in Sec61 translocon alpha 1 subunit (SEC61A1). J Allergy Clin Immunol 2018;141: 1427–38.
44. Fischbach H, Döring M, Nikles D, Lehnert E, Baldauf C, Kalinke U, et al. Ultrasensitive quantification of TAP-dependent antigen compartmentalization in scarce primary immune cell subsets. Nat Commun 2015;6:6199.
45. Grossmann N, Vakkasoglu AS, Hulpke S, Abele R, Gaudet R, Tampé R. Mechanistic determinants of the directionality and energetics of active export by a heterodimeric ABC transporter. Nat Commun 2014;5:5419.
46. Blees A, Reichel K, Trowitzsch S, Fisette O, Bock C, Abele R, et al. Assembly of the MHC I peptide-loading complex determined by a conserved ionic lock-switch. Sci Rep 2015;5:17341.
47. Kelly A, Powis SH, Kerr LA, Mockridge I, Elliott T, Bastin J, et al. Assembly and function of the two ABC transporter proteins encoded in the human major histocompatibility complex. Nature 1992;355:641–4.
48. Borsche M, Pereira SL, Klein C, Grünewald A. Mitochondria and Parkinson's disease: clinical, molecular, and translational aspects. J Parkinsons Dis 2021;11:45–60.
49. Jodeiri Farshbaf M, Ghaedi K. Huntington's disease and mitochondria. Neurotox Res 2017;32:518–29.
50. Sawant N, Morton H, Kshirsagar S, Reddy AP, Reddy PH. Mitochondrial abnormalities and synaptic damage in Huntington's disease: a focus on defective mitophagy and mitochondria-targeted therapeutics. Mol Neurobiol 2021;58: 6350–77.
51. Stürzl M, Kunz M, Krug SM, Naschberger E. Angiocrine regulation of epithelial barrier integrity in inflammatory bowel disease. Front Med 2021;8:643607.
52. Herrero R, Sanchez G, Lorente JA. New insights into the mechanisms of pulmonary edema in acute lung injury. Ann Transl Med 2018;6:32.
53. Goh KJ, Choong MC, Cheong EH, Kalimuddin S, Duu Wen S, Phua GC, et al. Rapid progression to acute respiratory distress syndrome: review of current understanding of critical illness from coronavirus disease 2019 (COVID-19) infection. Ann Acad Med Singapore 2020;49:108–18.
54. Wittekindt OH. Tight junctions in pulmonary epithelia during lung inflammation. Pflügers Archiv 2017;469:135–47.
55. Sawada N. Tight junction-related human diseases. Pathol Int 2013;63:1–12.

56. Blasig IE, Haseloff RF. Tight junctions and tissue barriers. Antioxid Redox Signal 2011;15:1163–6.
57. Marzesco AM, Dunia I, Pandjaitan R, Recouvreur M, Dauzonne D, Benedetti EL, et al. The small GTPase Rab13 regulates assembly of functional tight junctions in epithelial cells. Mol Biol Cell 2002;13:1819–31.
58. Köhler K, Louvard D, Zahraoui A. Rab13 regulates PKA signaling during tight junction assembly. J Cell Biol 2004;165:175–80.
59. Morimoto S, Nishimura N, Terai T, Manabe S, Yamamoto Y, Shinahara W, et al. Rab13 mediates the continuous endocytic recycling of occludin to the cell surface. J Biol Chem 2005;280: 2220–8.
60. Zahraoui A, Joberty G, Arpin M, Fontaine JJ, Hellio R, Tavitian A, et al. A small rab GTPase is distributed in cytoplasmic vesicles in non polarized cells but colocalizes with the tight junction marker ZO-1 in polarized epithelial cells. J Cell Biol 1994;124:101–15.
61. Kolev NG, Steitz JA. Symplekin and multiple other polyadenylation factors participate in 3′-end maturation of histone mRNAs. Genes Dev 2005;19:2583–92.
62. Xiang K, Nagaike T, Xiang S, Kilic T, Beh MM, Manley JL, et al. Crystal structure of the human symplekin-Ssu72-CTD phosphopeptide complex. Nature 2010;467:729–33.
63. Perez White BE, Ventrella R, Kaplan N, Cable CJ, Thomas PM, Getsios S. EphA2 proteomics in human keratinocytes reveals a novel association with afadin and epidermal tight junctions. J Cell Sci 2017;130:111–8.
64. Kirchner F, Schuetz A, Boldt LH, Martens K, Dittmar G, Haverkamp W, et al. Molecular insights into arrhythmogenic right ventricular cardiomyopathy caused by plakophilin-2 missense mutations. Circ Cardiovasc Genet 2012;5:400–11.
65. Istvan ES, Deisenhofer J. Structural mechanism for statin inhibition of HMG-CoA reductase. Science 2001;292:1160–4.
66. Sarver RW, Bills E, Bolton G, Bratton LD, Caspers NL, Dunbar JB, et al. Thermodynamic and structure guided design of statin based inhibitors of 3-hydroxy-3-methylglutaryl coenzyme A reductase. J Med Chem 2008;51:3804–13.
67. Luskey KL, Stevens B. Human 3-hydroxy-3-methylglutaryl coenzyme A reductase. Conserved domains responsible for catalytic activity and sterol-regulated degradation. J Biol Chem 1985;260:10271–7.
68. Cuccioloni M, Mozzicafreddo M, Spina M, Tran CN, Falconi M, Eleuteri AM, et al. Epigallocatechin-3-gallate potently inhibits the in vitro activity of hydroxy-3-methyl-glutaryl-CoA reductase. J Lipid Res 2011;52:897–907.
69. Brown MS, Goldstein JL. Multivalent feedback regulation of HMG CoA reductase, a control mechanism coordinating isoprenoid synthesis and cell growth. J Lipid Res 1980;21:505–17.
70. Zanoni P, Khetarpal SA, Larach DB, Hancock-Cerutti WF, Millar JS, Cuchel M, et al. Rare variant in scavenger receptor BI raises HDL cholesterol and increases risk of coronary heart disease. Science 2016;351:1166–71.
71. Seidah NG, Poirier S, Denis M, Parker R, Miao B, Mapelli C, et al. Annexin A2 is a natural extrahepatic inhibitor of the PCSK9-induced LDL receptor degradation. PLoS One 2012;7:e41865.
72. de Marco MC, Kremer L, Albar JP, Martinez-Menarguez JA, Ballesta J, Garcia-Lopez MA, et al. BENE, a novel raft-associated protein of the MAL proteolipid family, interacts with caveolin-1 in human endothelial-like ECV304 cells. J Biol Chem 2001;276: 23009–17.
73. Gaudet P, Livstone MS, Lewis SE, Thomas PD. Phylogenetic-based propagation of functional annotations within the Gene Ontology consortium. Brief Bioinform 2011;12:449–62.
74. Waterham HR, Koster J, Romeijn GJ, Hennekam RC, Vreken P, Andersson HC, et al. Mutations in the 3beta-hydroxysterol Delta24-reductase gene cause desmosterolosis, an autosomal recessive disorder of cholesterol biosynthesis. Am J Hum Genet 2001;69:685–94.
75. Schaaf CP, Koster J, Katsonis P, Kratz L, Shchelochkov OA, Scaglia F, et al. Desmosterolosis-phenotypic and molecular characterization of a third case and review of the literature. Am J Med Genet A 2011;155:1597–604.
76. Luu W, Hart-Smith G, Sharpe LJ, Brown AJ. The terminal enzymes of cholesterol synthesis, DHCR24 and DHCR7, interact physically and functionally. J Lipid Res 2015;56:888–97.
77. Zerenturk EJ, Kristiana I, Gill S, Brown AJ. The endogenous regulator 24(S),25-epoxycholesterol inhibits cholesterol synthesis at DHCR24 (Seladin-1). Biochim Biophys Acta 2012; 1821:1269–77.
78. Moebius FF, Fitzky BU, Lee JN, Paik YK, Glossmann H. Molecular cloning and expression of the human delta7-sterol reductase. Proc Natl Acad Sci U S A 1998;95:1899–902.
79. Wassif CA, Maslen C, Kachilele-Linjewile S, Lin D, Linck LM, Connor WE, et al. Mutations in the human sterol delta7-reductase gene at 11q12-13 cause Smith-Lemli-Opitz syndrome. Am J Hum Genet 1998;63:55–62.
80. Rajavashisth TB, Taylor AK, Andalibi A, Svenson KL, Lusis AJ. Identification of a zinc finger protein that binds to the sterol regulatory element. Science 1989;245:640–3.
81. Huber MD, Vesely PW, Datta K, Gerace L. Erlins restrict SREBP activation in the ER and regulate cellular cholesterol homeostasis. J Cell Biol 2013;203:427–36.
82. Lin J, Lin S, Choy PC, Shen X, Deng C, Kuang S, et al. The regulation of the cardiac potassium channel (HERG) by caveolin-1. Biochem Cell Biol 2008;86:405–15.
83. Roberts JD, Herkert JC, Rutberg J, Nikkel SM, Wiesfeld AC, Dooijes D, et al. Detection of genomic deletions of PKP2 in arrhythmogenic right ventricular cardiomyopathy. Clin Genet 2013;83:452–6.
84. Cheung JY, Zhang XQ, Song J, Gao E, Chan TO, Rabinowitz JE, et al. Coordinated regulation of cardiac Na(+)/Ca (2+) exchanger and Na (+)-K (+)-ATPase by phospholemman (FXYD1). Adv Exp Med Biol 2013;961:175–90.
85. Nyegaard M, Overgaard MT, Søndergaard MT, Vranas M, Behr ER, Hildebrandt LL, et al. Mutations in calmodulin cause ventricular tachycardia and sudden cardiac death. Am J Hum Genet 2012;91:703–12.
86. Karibe A, Tobacman LS, Strand J, Butters C, Back N, Bachinski LL, et al. Hypertrophic cardiomyopathy caused by a novel alpha-tropomyosin mutation (V95A) is associated with mild cardiac phenotype, abnormal calcium binding to troponin, abnormal myosin cycling, and poor prognosis. Circulation 2001;103:65–71.
87. Holt I, Clements L, Manilal S, Morris GE. How does a g993t mutation in the emerin gene cause Emery-Dreifuss muscular dystrophy? Biochem Biophys Res Commun 2001;287:1129–33.

88. Fishman GI, Spray DC, Leinwand LA. Molecular characterization and functional expression of the human cardiac gap junction channel. J Cell Biol 1990;111:589–98.
89. Pilichou K, Nava A, Basso C, Beffagna G, Bauce B, Lorenzon A, et al. Mutations in desmoglein-2 gene are associated with arrhythmogenic right ventricular cardiomyopathy. Circulation 2006;113:1171–9.
90. Rasmussen TB, Palmfeldt J, Nissen PH, Magnoni R, Dalager S, Jensen UB, et al. Mutated desmoglein-2 proteins are incorporated into desmosomes and exhibit dominant-negative effects in arrhythmogenic right ventricular cardiomyopathy. Hum Mutat 2013;34:697–705.
91. Rampazzo A, Nava A, Malacrida S, Beffagna G, Bauce B, Rossi V, et al. Mutation in human desmoplakin domain binding to plakoglobin causes a dominant form of arrhythmogenic right ventricular cardiomyopathy. Am J Hum Genet 2002;71:1200–6.
92. Barwe SP, Jordan MC, Skay A, Inge L, Rajasekaran SA, Wolle D, et al. Dysfunction of ouabain-induced cardiac contractility in mice with heart-specific ablation of Na,K-ATPase beta1-subunit. J Mol Cell Cardiol 2009;47:552–60.
93. Fatkin D, MacRae C, Sasaki T, Wolff MR, Porcu M, Frenneaux M, et al. Missense mutations in the rod domain of the lamin A/C gene as causes of dilated cardiomyopathy and conduction-system disease. N Engl J Med 1999;341:1715–24.
94. Chen L, Lee L, Kudlow BA, Dos Santos HG, Sletvold O, Shafeghati Y, et al. LMNA mutations in atypical Werner's syndrome. Lancet 2003;362:440–5.
95. Renou L, Stora S, Yaou RB, Volk M, Sinkovec M, Demay L, et al. Heart-hand syndrome of Slovenian type: a new kind of laminopathy. J Med Genet 2008;45:666–71.
96. Kane MS, Lindsay ME, Judge DP, Barrowman J, Ap Rhys C, Simonson L, et al. LMNA-associated cardiocutaneous progeria: an inherited autosomal dominant premature aging syndrome with late onset. Am J Med Genet A 2013;161:1599–611.
97. Ekhteraei-Tousi S, Mohammad-Soltani B, Sadeghizadeh M, Mowla SJ, Parsi S, Soleimani M. Inhibitory effect of hsa-miR-590-5p on cardiosphere-derived stem cells differentiation through downregulation of TGFB signaling. J Cell Biochem 2015;116:179–91.
98. Singla DK, Sun B. Transforming growth factor-beta2 enhances differentiation of cardiac myocytes from embryonic stem cells. Biochem Biophys Res Commun 2005;332:135–41.
99. Chen Y, Zhang N, Zhang J, Guo J, Dong S, Sun H, et al. Immune response pattern across the asymptomatic, symptomatic and convalescent periods of COVID-19. Biochim Biophys Acta, Proteins Proteomics 2022;1870:140736.
100. Tian W, Zhang N, Jin R, Feng Y, Wang S, Gao S, et al. Immune suppression in the early stage of COVID-19 disease. Nat Commun 2020;11:5859.
101. Chen Y, Yao H, Zhang N, Wu J, Gao S, Guo J, et al. Proteomic analysis identifies prolonged disturbances in pathways related to cholesterol metabolism and myocardium function in the COVID-19 recovery stage. J Proteome Res 2021;20:3463–74.
102. Walker JR, Corpina RA, Goldberg J. Structure of the Ku heterodimer bound to DNA and its implications for double-strand break repair. Nature 2001;412:607–14.
103. Rana R, Rathi V, Ganguly NK. A comprehensive overview of proteomics approach for COVID 19: new perspectives in target therapy strategies. J Proteins Proteom 2020;11:223–32.
104. Sood S, Aggarwal V, Aggarwal D, Upadhyay SK, Sak K, Tuli HS, et al. COVID-19 pandemic: from molecular biology, pathogenesis, detection, and treatment to global societal impact. Curr Pharmacol Rep 2020;6:212–27.
105. Whetton AD, Preston GW, Abubeker S, Geifman N. Proteomics and informatics for understanding phases and identifying biomarkers in COVID-19 disease. J Proteome Res 2020;19:4219–32.
106. Ong EZ, Chan YFZ, Leong WY, Lee NMY, Kalimuddin S, Haja Mohideen SM, et al. A dynamic immune response shapes COVID-19 progression. Cell Host Microbe 2020;27:879–82.e2.
107. Wilk AJ, Rustagi A, Zhao NQ, Roque J, Martínez-Colón GJ, McKechnie JL, et al. A single-cell atlas of the peripheral immune response in patients with severe COVID-19. Nat Med 2020;26:1070–6.
108. Catanzaro M, Fagiani F, Racchi M, Corsini E, Govoni S, Lanni C. Immune response in COVID-19: addressing a pharmacological challenge by targeting pathways triggered by SARS-CoV-2. Signal Transduct Target Ther 2020;5:84.
109. Zhu L, Yang P, Zhao Y, Zhuang Z, Wang Z, Song R, et al. Single-cell sequencing of peripheral mononuclear cells reveals distinct immune response landscapes of COVID-19 and influenza patients. Immunity 2020;53:685–96.e3.
110. Campbell JS, Hallett MB. Active calpain in phagocytically competent human neutrophils: electroinjection of fluorogenic calpain substrate. Biochem Biophys Res Commun 2015;457:341–6.
111. Wu C, Chen X, Cai Y, Xia J, Zhou X, Xu S, et al. Risk factors associated with acute respiratory distress syndrome and death in patients with coronavirus disease 2019 pneumonia in Wuhan, China. JAMA Intern Med 2020;180:934–43.
112. Kuri-Cervantes L, Pampena MB, Meng W, Rosenfeld AM, Ittner CAG, Weisman AR, et al. Comprehensive mapping of immune perturbations associated with severe COVID-19. Sci Immunol 2020;5:eabd7114.
113. Tan L, Wang Q, Zhang D, Ding J, Huang Q, Tang YQ, et al. Lymphopenia predicts disease severity of COVID-19: a descriptive and predictive study. Signal Transduct Target Ther 2020;5:33.
114. Huang C, Wang Y, Li X, Ren L, Zhao J, Hu Y, et al. Clinical features of patients infected with 2019 novel coronavirus in Wuhan, China. Lancet 2020;395:497–506.
115. Zheng M, Gao Y, Wang G, Song G, Liu S, Sun D, et al. Functional exhaustion of antiviral lymphocytes in COVID-19 patients. Cell Mol Immunol 2020;17:533–5.
116. Bankar R, Suvarna K, Ghantasala S, Banerjee A, Biswas D, Choudhury M, et al. Proteomic investigation reveals dominant alterations of neutrophil degranulation and mRNA translation pathways in patients with COVID-19. iScience 2021;24:102135.
117. Watari K, Shibata T, Nabeshima H, Shinoda A, Fukunaga Y, Kawahara A, et al. Impaired differentiation of macrophage lineage cells attenuates bone remodeling and inflammatory angiogenesis in Ndrg1 deficient mice. Sci Rep 2016;6:19470.
118. Vandenbark AA, Meza-Romero R, Offner H. Surviving the storm: dealing with COVID-19. Cell Immunol 2020;354:104153.
119. Begue F, Tanaka S, Mouktadi Z, Rondeau P, Veeren B, Diotel N, et al. Altered high-density lipoprotein composition and functions during severe COVID-19. Sci Rep 2021;11:2291.
120. Puntmann VO, Carerj ML, Wieters I, Fahim M, Arendt C, Hoffmann J, et al. Outcomes of cardiovascular magnetic resonance

imaging in patients recently recovered from coronavirus disease 2019 (COVID-19). JAMA Cardiol 2020;5:1265–73.
121. Doykov I, Hällqvist J, Gilmour KC, Grandjean L, Mills K, Heywood WE. 'The long tail of Covid-19' – the detection of a prolonged inflammatory response after a SARS-CoV-2 infection in asymptomatic and mildly affected patients. F1000Res 2020;9: 1349.
122. De Felice FG, Tovar-Moll F, Moll J, Munoz DP, Ferreira ST. Severe acute respiratory syndrome coronavirus 2 (SARS-CoV-2) and the central nervous system. Trends Neurosci 2020;43:355–7.
123. Varga Z, Flammer AJ, Steiger P, Haberecker M, Andermatt R, Zinkernagel AS, et al. Endothelial cell infection and endotheliitis in COVID-19. Lancet 2020;395:1417–8.
124. Zhang C, Shi L, Wang FS. Liver injury in COVID-19: management and challenges. Lancet Gastroenterol Hepatol 2020;5:428–30.
125. McArdle A, Washington KE, Chazarin Orgel B, Binek A, Manalo DM, Rivas A, et al. Discovery proteomics for COVID-19: where we are now. J Proteome Res 2021;20:4627–39.
126. Xu Y, Schnorrer P, Proietto A, Kowalski G, Febbraio MA, Acha-Orbea H, et al. IL-10 controls cystatin C synthesis and blood concentration in response to inflammation through regulation of IFN regulatory factor 8 expression. J Immunol 2011;186:3666–73.
127. Matsubara T, Mita A, Minami K, Hosooka T, Kitazawa S, Takahashi K, et al. PGRN is a key adipokine mediating high fat diet-induced insulin resistance and obesity through IL-6 in adipose tissue. Cell Metab 2012;15:38–50.
128. Leng L, Cao R, Ma J, Mou D, Zhu Y, Li W, et al. Pathological features of COVID-19-associated lung injury: a preliminary proteomics report based on clinical samples. Signal Transduct Target Ther 2020;5:240.